2184

NASA CR-134589

Department of Aerospace Engineering

University of Cincinnati

EROSION IN RADIAL INFLOW TURBINES - VOLUME I: EROSIVE PARTICLE TRAJECTORY SIMILARITY

By:

W.B. Clevenger, Jr.

and

W. Tabakoff

Supported by:

NATIONAL AERONAUTICS AND SPACE ADMINISTRATION

Lewis Research Center

Contract NGR 36-004-055

1. Report No.	2. Government Accession No.	3. Recipient's Catalog No.
NASA CR 134589		

4. Title and Subtitle	5. Report Date
Erosion in Radial Inflow Turbines - Volume I: Erosive Particle Trajectory Similarity	February 1974
	6. Performing Organization Code
7. Author(s)	8. Performing Organization Report No.
W.B. Clevenger, Jr. and W. Tabakoff	
	10. Work Unit No.
9. Performing Organization Name and Address	11. Contract or Grant No.
Department of Aerospace Engineering University of Cincinnati Cincinnati, Ohio 45221	NGR 36-004-055
	13. Type of Report and Period Covered
12. Sponsoring Agency Name and Address	Contractor Report
National Aeronautics and Space Administration Washington, D.C. 20546	14. Sponsoring Agency Code

15. Supplementary Notes

Final Report. Project Manager, Jeffrey E. Haas, Fluid Systems Components Division, NASA, Lewis Research Center, Cleveland, Ohio 44135

16. Abstract

This report derives similarity parameters from the equations of motion of particles immersed in a gas flow. These parameters relate the particles which follow a certain trajectory in an equivalent cold gas turbine to particles that will follow the same trajectory in a real hot gas turbine. Numerical solutions of the trajectories that particles follow in the vortex and rotor regions of a radial inflow turbine are used to verify the range of Reynolds numbers in which the derived similarity parameters are applicable. In addition, an example is presented of typical particle sizes that can be observed in high speed photographic data collection and at the same time simulate the trajectories of particles in a real hot gas turbine.

17. Key Words (Suggested by Author(s))	18. Distribution Statement
Radial Turbine Erosion Similarity Particulated Flow	Unclassified - unlimited

19. Security Classif. (of this report)	20. Security Classif. (of this page)	21. No. of Pages	22. Price*
Unclassified	Unclassified	53	$3.00

* For sale by the National Technical Information Service, Springfield, Virginia 22151

NASA CR-134589

EROSION IN RADIAL INFLOW TURBINES - VOLUME I: EROSIVE PARTICLE TRAJECTORY SIMILARITY

By:

W.B. Clevenger, Jr.

and

W. Tabakoff

Supported by:

NATIONAL AERONAUTICS AND SPACE ADMINISTRATION

Lewis Research Center

Contract NGR 36-004-055

TABLE OF CONTENTS

SUMMARY

The equations of motion of particles immersed in a gas flow are used as the basis for determining two similarity parameters which are applicable to different Reynolds number ranges. Of these two similarity parameters, only one, a characteristic length, generally applies to the range of Reynolds number that are experienced by most particles large enough to cause erosion problems.

The two-dimensional gas flow in an inward flowing vortex is used as the basis for a study of the applicability of the characteristic length. A large number of combinations of particle sizes, densities, and gas flow properties were investigated to determine the range of Reynolds numbers within which the characteristic length is applicable. The results of this study reveal that precise trajectory similarity can be achieved with Reynolds numbers greater than 500.

The three-dimensional gas flow in a radial inflow turbine rotor is used as the basis for comparing trajectories of similar particles in more complicated flows. Most of the particle trajectory cases considered in this study had Reynolds numbers below 500, but the results indicated that similar particles still followed the same general trajectory through the rotor, even though they did not follow the same precise trajectory. This indicates that the characteristic length is a useful similarity parameter for studying the trends in erosive particle trajectories without regard to Reynolds number limitations.

INTRODUCTION

The purpose of this study is to investigate the erosion phenomena in radial inflow turbines and to study ways of eliminating this erosion. The overall study includes an investigation of erosive particle trajectory similarity, investigation of the balance between radial aerodynamic and centrifugal forces acting on the particles, a review of the phenomena of erosion of blade materials by the action of particles, and an investigation of the trajectories that particles follow as they pass through a radial inflow turbine. The results of these investigations will be published in a series of four volumes which will generally cover the topics indicated. A fifth volume will present the computer programs that were developed as part of this research.

Small radial inflow turbines have the potential of higher efficiencies than small axial flow turbines of approximately the same size. This advantage makes it worthwhile to investigate phenomena that may have significant effects on the performance of such engines.

In recent times, the problem of particle erosion has become important due to the significant decreases in the rated operating lifetimes of gas turbine engines which are used in dusty environments. The most significant affects of erosion have been observed on active military helicopters, where operations at low altitudes and remote landing fields have greatly increased the number of particles that enter the engines. Although these helicopters have main engines which utilize axial flow turbines, some also have auxiliary engines used as power sources for special devices, which utilize radial turbines, as shown schematically in Figure 1. Radial inflow turbines have also been used on small portable power plants which also are likely to be used in areas where dust ingestion will occur. In addition, radial inflow turbines have long been used in turbo-chargers on reciprocating engines, and are seriously being considered for future use in transportation vehicles such as trucks and automobiles.

These radial turbine engines have, however, a more serious erosion problem than axial flow turbines because larger particles experience a radially outward centrifugal force that is greater than the radially inward component of the aerodynamic drag force. This causes each of these larger particles to strike the stator and rotor blades many times thus causing a significantly greater amount of erosion than occurs when each particle strikes the blade surfaces only a few times as in an axial flow turbine.

The reason for determining similarity parameters is that a great deal of experimental research in turbines is done with air at pressures and temperatures that are relatively low compared to the actual operating conditions of a real turbine. Experimental data for turbines is then evaluated in terms of corrected performance parameters that relate the energy output, rotating speed, pressure ratio, torque and air flow rate to the performance parameters that occur if the inlet air to the turbine had been standard sea level air. Data in this form can then be used to predict the performance of equivalent hot air turbines which have the same geometric shapes and sizes but significantly different pressures, temperatures and gas properties. In addition, much of the experimental data for the trajectories of particles in two-dimensional cascades has been obtained using equivalent cold air wind tunnels.

Because of the large differences in flow properties between the cold air tests and the actual hot air cases, the trajectories of particles of equal density and size will probably change between the two cases. Thus, it becomes worthwhile to determine the relationships of certain parameters which can be grouped together so that particles used in cold flow turbines and cascades can be defined such that their trajectories will be similar to those of real particles in equivalent hot flow applications.

There have been many reports published in recent literature dealing with the problems of dust erosion in gas turbine engines. The references listed in this volume are part of a larger list of publications that were reviewed as part of the overall research project. Only those papers with results which are of interest in

this particular investigation are included. Subsequent volumes will include additional papers that are pertinent to those particular investigations.

References 1 through 5 constitute a comprehensive review of the problem of erosive particle trajectories in axial flow cascades. These reports all deal with the trajectory patterns that particles follow, based on analytical results for several hot air flows and generally based on experimental results for the equivalent cold air flows. The studies include variations caused by differences in most particle and gas flow properties.

Another comprehensive study of the erosion problem is presented in References 6 through 9. This study takes a slightly different approach by concentrating more on predicting the amount and location that erosion damage will occur in less complicated blading configurations. Experimental data on particle trajectories is included in these reports.

Reference 10 reports the results for an experimental study of several ways that seemed promising in reducing the amount of erosion that occurs in radial turbines. This report does not consider trajectories, other than a few straight line trajectories as particles leave the rotor.

Reference 11 contains an analytical study of the trajectories of particles in the inlet region of the radial turbine. This author includes some techniques for reducing the amount of erosion and considers the affects of these changes analytically.

Reference 12 discusses the acceleration of a spherical particle in a uniform gas flow, and in this parametric study, a grouping of constants is done to facilitate the solution of the equations of motion in a one-dimensional flow field. This work is more generally applicable to rocket nozzles where particle interaction with surfaces may possibly be neglected. The variable groupings reported in this work are similar to those that are developed here.

Finally, it should be stated that the similarity parameters that are indicated here reduce the number of variables that must

be considered in analytically studying the trajectories of erosive particles in turbomachinery, and also provide the basis for extending experimental results of particle trajectories to real hot gas cases without the need to build hot gas test facilities.

ANALYSIS

Equivalent Turbines

Much experimental research in turbines is done with air at pressures and temperatures that are relatively low compared to the actual operating conditions of a real turbine. Experimental data is then evaluated in terms of corrected performance parameters that relate the energy output, rotating speed, and air flow rate to the parameters that occur if the inlet air to the turbine had been standard sea level air.

These parameters can be found by comparing the actual conditions that occur in a turbine to the conditions that occur when sea level air is used, with the velocity of the air near the critical velocity in both cases. Usually geometric dimensions, blade shapes, the gas dimensionless velocity, V/V_{cr}, and the velocity directions are assumed to be unchanged between the hot air turbine and the cold air equivalent turbine.

Using these assumptions, the corrected performance parameters are determined to be as follows.[13]

weight flow $$\frac{\dot{w}\sqrt{\theta_{cr}}}{\delta} \quad \varepsilon \tag{1}$$

work energy $$\frac{\Delta h}{\theta_{cr}} \tag{2}$$

rotating speed $$\frac{N}{\sqrt{\theta_{cr}}} \tag{3}$$

Correction of performance measurements in terms of these parameters provides a useful way for comparing data from different

turbines and is extremely useful in predicting the performance of a turbine when it is not feasible to build the actual hot air turbine in an experimental study. In the discussion that follows, we will have occasion to recall the basic assumptions used in developing these parameters. These basic assumptions were that the geometric shapes and dimensions of the two equivalent turbines were the same, and that the dimensionless speeds, are equivalent in both cases and approximately equal to 1 throughout the turbine.

Particle Equations of Motion

The equations of motion of a particle in a rotating reference frame must be derived and understood if the trajectories of particles in turbine rotors is to be determined numerically. In addition, these equations are the basis upon which similarity parameters and related terms are derived.

The equations of motion of a particle in a cylindrical coordinate system offers a basis for determining the parameters that will be most influential in determining the properties of particles that will have similar trajectories. The most general case will be that of the dynamic equations of three-dimensional particle motion in a rotating reference frame. Figure 2 illustrates the coordinate system used throughout this report.

For the case of steady rotation about the z-axis with a rotating speed, ω, the acceleration vector is,

$$\bar{a} = \frac{d^2\bar{r}}{dt^2} = \left[\frac{\delta^2 r}{\delta t^2} - r\left(\frac{\delta\theta}{\delta t}\right)^2 - 2\, r\, \omega\, \frac{\delta\theta}{\delta t} - r\, \omega^2\right] \bar{e}_r$$

$$+ \left[r\, \frac{\delta^2\theta}{\delta t^2} + 2\, \frac{\delta r}{\delta t}\, \frac{\delta\theta}{\delta t} + 2\, \omega\, \frac{\delta r}{\delta t}\right] \bar{e}_\theta$$

$$+ \frac{\delta^2 z}{\delta t^2}\, \bar{e}_z \qquad (4)$$

where $\delta/\delta t$ represents the time rate of change of r, θ, or z with respect to the rotating reference frame.

Newton's Second Law, $\bar{F} = m\bar{a}$, is used to relate the acceleration vector experienced by the particle and the resultant force that acts on the particle.

The forces that act on a particle include aerodynamic forces, gravitational forces, and electrostatic forces if the particle carries a charge. Electrostatic forces on charged particles can in some cases be quite significant in affecting the trajectories of the particles. However, to be significant, additional devices would have to be added to a turbine engine to generate an electric field within parts of the flow passage, and to charge the particles in some way. Because such devices are beyond the scope of this project, electrostatic forces will be neglected.

Gravity forces will also be neglected in this part of the overall study. Generally, the influence of gravity on a particle trajectory will be quite small because of the relatively short time that the particle travels in the turbine. In the scroll, the dwell time of the particles is sufficiently long to warrant consideration of gravitational effects. But in the vortex and rotor analysis as are done in this volume of the report, the gravitational acceleration is neglected.

For nonspherical particles, the aerodynamic forces will include drag, lift, and moment forces. Because most particles will spin rather than remain at some definable angle of attack, moment and lift forces are neglected and only drag forces are considered. This drag force acts in the direction of the air velocity with respect to the particle velocity, and is given by

$$D = \frac{1}{2} \rho \bar{V}^2 A C_D \left[\frac{V_r}{|\bar{V}|} \bar{e}_r + \frac{V_\theta}{|\bar{V}|} \bar{e}_\theta + \frac{V_z}{|\bar{V}|} \bar{e}_z \right] \tag{5}$$

where

$$\bar{V} = V_r \bar{e}_r + V_\theta \bar{e}_\theta + V_z \bar{e}_z \tag{6}$$

is the relative velocity of the gas with respect to the particle.

The components of this relative velocity vector are

$$V_r = v_r - \frac{\delta r}{\delta t}$$

$$V_\theta = v_u - r\,\frac{\delta \theta}{\delta t}$$

$$V_z = v_z - \frac{\delta z}{\delta t} \qquad (7)$$

where v_r, v_u, v_z are respectively the radial, tangential and axial components of the gas in the rotating reference frame in the most general case, and $\delta r/\delta t$, $r\,\delta\theta/\delta t$, and $\delta z/\delta t$ are respectively the radial, tangential and axial velocity components of the particle. It should be noted that when ω in Equation (4) is zero, corresponding to no rotation of the reference frame, the relative velocities v_r, v_u, and v_z become absolute velocities.

Collecting the components of the acceleration and drag through Newton's Law yields

$$\frac{\delta^2 r}{\delta t^2} - r\,\left(\frac{\delta\theta}{\delta t}\right)^2 - 2\,r\,\omega\,\frac{\delta\theta}{\delta t} - r\,\omega^2 = \frac{1}{2}\,\frac{\rho V^2 A C_D}{m}\,\frac{V_r}{|\bar{V}|} \qquad (8a)$$

$$r\,\frac{\delta^2\theta}{\delta t^2} + 2\,\frac{\delta r}{\delta t}\,\frac{\delta\theta}{\delta t} + 2\,\omega\,\frac{\delta r}{\delta t} = \frac{1}{2}\,\frac{\rho V^2 A C_D}{m}\,\frac{V_\theta}{|\bar{V}|} \qquad (8b)$$

$$\frac{\delta^2 z}{\delta t^2} = \frac{1}{2}\,\frac{\rho V^2 A C_D}{m}\,\frac{V_z}{|\bar{V}|} \qquad (8c)$$

The drag coefficient of a spherical particle is well established experimentally over a large range of Reynolds numbers. Because of the significance of C_D in Equation (8), a description of C_D in algebraic form is necessary for the numerical solution of the particle trajectory. The value of C_D was determined by using the following relations.

$$C_D = 4.5 + \frac{24}{Re} \qquad Re < 1.0 \qquad (9a)$$

$$C_D = 28.5 - 24.0\ (\text{Log Re}) + 9.0682\ (\text{Log Re})^2$$

$$- 1.7713\ (\text{Log Re})^3 + 0.1718\ (\text{Log Re})^4 - 0.0065\ (\text{Log Re})^5$$

$$1.0 < \text{Re} < 3000 \qquad (9b)$$

$$C_D = 0.4 \qquad 3000 < \text{Re} < 2.5 \times 10^{-5} \qquad (9c)$$

These formulas were based on drag coefficient versus Reynolds number data such as contained in many text books.

Equation (8) is integrated numerically to yield the motion of a particle in a rotating reference frame.

Similarity Parameters

Similarity parameters allow the grouping of the important variables that influence trajectories and reduce the number of individual cases that must be studied, as well as allowing the application of the results presented to other similar radial inflow turbines.

As an example of the variations that can occur, Figure 3 indicates the trajectories that a 100 micron particle will follow in the inward flowing vortex. The particle had a specific gravity of one. Several different values of initial velocity were used. As would be expected, the particles having the greater inlet velocities tended to travel in straighter trajectories and be less influenced by the gas flow than the particles that had the slower velocity. Of perhaps greater significance though is the fact that even this relatively massive partice has a different trajectory in the cold air flow than in the hot air flow. The large differences in the trajectories of these two cases indicates the need to determine what similarity parameters might be obtained to compare the trajectories in hot and cold air turbines.

Neglecting all but the aerodynamic drag force that acts on the particle, then Newton's Second Law is

$$\bar{D} = m\,\bar{a} \qquad (10)$$

where $\bar{D}$ is the drag force, m is the particle mass, and $\bar{a}$ is the acceleration.

The drag can be expressed in scalar form as

$$D = \frac{1}{2} \rho_g V^2 A_p C_D \tag{11}$$

Treating the particle as a spherical particle, then the mass is the density times the volume of a sphere, the area in Equation (11) is the area of a circle, and letting $C_D = 0.4$, then the acceleration becomes

$$a = \frac{3}{10} \frac{\rho_g V^2}{\rho_p D_p} \tag{12}$$

Defining the characteristic length as

$$\delta = \frac{10}{3} \frac{\rho_p D_p}{\rho_g} \tag{13}$$

then

$$a = \frac{V^2}{\delta} \tag{14}$$

In the theory of equivalent flows in turbines, the velocity is always assumed to be near the sonic velocity, which causes the gas properties to be near their critical values. In order to maintain consistency with the ideas of equivalent flow fields, the gas density, ρ_g, in Equation (13) can be chosen to represent the critical density of the gas. When this is done in this report, the characteristic length is referred to as the critical characteristic length, δ^*.

For particles where the Reynolds number tends to be less than one, the expression $C_D = 24/Re$ can be substituted into Equation (11). When this is done, the acceleration becomes

$$a = \frac{18 \mu_g}{\rho_p D_p^2} |V| \tag{15}$$

Defining the time constant

$$\tau = \frac{\rho_p D_p^2}{18 \mu_g} \tag{16}$$

then

$$a = \frac{|V|}{\tau} \tag{17}$$

The gas viscosity is a function of temperature, and because of the large variations in temperature between the hot air turbine and the equivalent cold air turbine, there will be significant changes in this term. In order to mainatin consistency with the assumptions of equivalent gas flow, the temperature T^* corresponding to a sonic flow was chosen as the temperature upon which to base the viscosity. The symbol τ^* refers to the time constant evaluated under these circumstances.

The use of the time constant has limited value in erosion studies because it applies to small particles that tend to follow the streamlines quite closely and therefore do not cause significant amounts of erosion. However, the derivation of this term is presented here for completeness.

RESULTS, COMPARISONS AND DISCUSSION

Free Vortex

For the gas flow in an inward flowing vortex, a computer program was written to integrate the equations of motion of a particle, in order to describe the trajectory of a particle in such a flow field. With this program, a large number of cases with different gas properties and different particle properties could be studied. An inward flowing vortex with a $V/V_{cr} = 0.8$ at 70°, and an inlet radius of 8.649 cm was selected for comparison purposes. The cold air reference case was taken having an inlet stagnation temperature and pressure of 288.2°K at 1 atm.

Although no limits were placed on the diameter of the particles, restriction on the gas densities and allowable particle densities

were imposed because of practical limits on the size of these quantities. The gas density was restricted by a requirement that the maximum allowed total inlet pressure was 10 atm. For the hot air flow, this corresponds to a maximum total inlet density of 3.186 kg/m^3. The restriction on the maximum allowable particle density was set by requiring the specific gravity of the particle to be always less than 12. Reference to any physical properties handbook will indicate that most solids have specific gravities below 12, with a few substances exceeding this number.

Figure 4 indicates the trajectories that occur in an inward flowing vortex for a large number of different particle densities, particle diameters and air densities. The values of the variables that were used in this study are tabulated in Table 1. The value of $\delta^* = 42.7$ cm was held constant. This value of δ^* was based on a typical reference case for cold air, indicated by "Ref" in the table. As indicated by the figure, even though there was a large variation in the gas density, the particle density, and the particle diameter, there was very little variation in the trajectories of the particles, except for the one case in which the particle had an average Reynolds number less than 500.

The results indicated in Figure 4 correspond to a particle that had a velocity equal to 50% of the gas velocity. Similar studies were done with particles that had 100% of the gas velocity and zero velocity at the inlet, with the gas densities, particle density and particle diameters not changed from the values indicated in Table 1. The results of this study were the same, that is, even though there was a large variation in the gas density, the particl density, and the particle diameter, there was very little variation in the trajectories of the particle, except for the one case in which the particle had a Reynolds number less than 500.

Figure 5 shows the variation in Reynolds number along the trajectory for a typcial particle selected from Table 1. All other particles investigated exhibited the same shaped curve when the Reynolds number was plotted against the position. The

location where the particles passed out of the flow field and the Reynolds number at that location were plotted in Figure 6 to indicate the variation of exit position with exit Reynolds number for the three cases where the initial particle velocity was 100%, 50%, and 0% of the gas velocity. This figure indicates that for Reynolds number above 500, there was no significant variation in the exit positions, which corresponds to no significant variation in the trajectory.

Figure 7 indicates the trajectories that occurred in the inward flowing vortex for δ^* = 16.5 cm. The values of particle density, particle diameter, and gas density that were used in this study are tabulated in Table 2. In this case, the value of δ^* was based on a typical reference case for hot air, which is indicated by "Ref" in the table. As in the study where δ^* was 42.7 cm, this study indicates that there is very little variation in the trajectories, except for the smaller Reynolds numbers.

The results indicated in Figure 7 correspond to a particle that had a velocity equal to 50% of the gas velocity. Similar studies were done with particles that had 100% of the gas velocity and zero velocity at the inlet, with the gas densities, particle densities and particle diameters not changed from the values indicated in Table 2. The results of this study were the same as indicated in Figure 7, that is, there was little variation in the trajectories except for the particles having average Reynolds numbers less than 500.

Figures similar to Figures 5 and 6 were prepared and these figures indicated the same result, that is, that there was no significant change in the exit position of the particle except when the Reynolds number dropped below 500.

These results indicate that the critical characteristic length can be used to determine the variables that should be controlled in order to provide similar trajectories in hot air and equivalent cold air flows, if the particle Reynolds number is generally maintained above 500. As the particle Reynolds number tends to drop below 500, the trajectory tends to deviate from the similar trajectory.

For smaller diameter particles, the expression given by Equation (16) is applicable, because the Reynolds numbers experienced by these particles is usually relatively small. The gas viscosity in this equation is a function of temperature and because of the large variations in temperature between the hot air turbine and the equivalent cold air turbine, there will be significant changes in the gas viscosity.

Figure 8 shows the trajectory of a 1 micron particle in an inward flowing vortex. The value of τ^* was held constant at 1.47×10^{-7} seconds, and the values of the variables for the several cases that are represented in the figure are given in Table 3. All the cases are essentially the same with the maximum variation being 1.5% of the tip radius for all cases studied. The trajectory indicated is arbitrarily truncated at a radius corresponding to 0.7 of the tip radius.

The trajectories of 10 micron particles in an inward flowing vortex are shown in Figure 9. In this case $\tau^* = 1.57 \times 10^{-4}$ seconds, and the values of the variables are given in Table 4. For this larger particle, there is a general tendency of the trajectories to spread, indicating that the use of τ^* as a similarity parameter is limited to particle diameters of the sub-micron range.

Generally, particles of this size do not cause significant amounts of erosion because they tend to follow the streamlines of the flow quite closely and thus tend to turn with the fluid instead of striking the blade surfaces.

These results indicate that similar trajectories of small particles of about 1 micron size or smaller can be obtained by holding τ^* constant in the hot air flow and the equivalent cold air flow, as long as the Reynolds number is less than 1 over most of the trajectory.

Radial Turbine Rotor

In order to study the trajectory of the particle in the rotor, a current rotor design was selected and the quasi-orthogonal method was used to determine the flows that occur in the hot gas and the

equivalent cold gas flows. Figure 10 shows the velocity diagrams that correspond to the inlet and mean exit stations of the rotor. The inlet conditions of the hot gas were 1477.8°K and 8.55 atm. In the study of the trajectories in the cold air equivalent turbine, the inlet conditions were 288.2°K and 1 atm. There were twelve blades, with no splitters, and the hot gas case rotational speed was 70,000 rpm. The total efficiency of the turbine was taken at 88% for both the cold air and the hot air studies.

Figures 11 show three views of a streamline as it traverses the rotor blades. The solid streamline results from the hot air solution and the dashed streamline results from the equivalent cold air solution for this rotor. These two streamlines are not identical because the compressibility terms are slightly different due to the variation in the ratio of specific heats in the two cases. Figure 11a, which is a meridional view of the rotor blade, indicates that there is a tendency for the streamlines to shift upward near the rotor exit in the equivalent cold air flow. Figure 11b, which is a view along the axis of the rotor blade with respect to the rotating reference frame, illustrates the central stream surface that divides the blade to blade region of the rotor. At the leading edge of the rotor, the quasi-orthogonal solution bends this stream surface so that it matches the velocity diagram at the inlet. The next figure, Figure 11c, is an axial view of the rotor with respect to the absolute reference frame. This illustrates the greatest change in the streamlines that occurs in the two cases.

Figures 12 show the trajectories of several particles having $\delta^* = 25.9$ cm. Both hot air and cold air trajectories are indicated. Figure 12c shows the most informative view of the trajectories that occur in these cases. As indicated, the trajectory is such that the blade overtakes the particle that is moving at 50% of the inlet air velocity. Figure 12b indicates that there is a small deviation in the trajectory between the hot and cold air cases. The value of $\delta^* = 25.9$ cm corresponds to a 100 micron particle with a specific gravity of 1.0 in the hot gas flow. For both

the hot gas and cold gas flow the particle specific gravity was varied between 1.0 and 12.0 with the particle diameter made correspondingly smaller in each case studied. The slight variation that occurred seems to result from the Reynolds number of the particle in the cold air case being generally below 500 for most of the trajectory.

Figures 13a, b, c, show the trajectories of particles that had $\delta^* = 2.59$ cm, which corresponded to a particle with 10 microns and a specific gravity of 1.0 in the hot gas case. All of these trajectories exhibited Reynolds numbers below 500 and there was no similarity in the trajectories. These smaller particles tended to make several low angle bounces off the shroud. It should be noted though that these trajectories all tend to follow the same general trends in their trajectory, even though the trajectories are not identically the same. This extends somewhat the applicability of the characteristic length as a similar parameter because particles having the same values of characteristic length can be expected to follow the same trends in trajectories, even if these trajectories are not identical.

Figures 14a, b, c, show the trajectories of particles for $\delta^* = 0.259$ cm, which corresponded to a particle with diameter of 1 micron and a specific gravity of 1.0 in the hot gas case. Past experience would indicate that particles this small would follow the streamlines quite closely, as the figures indicate.

In summary, this section of the progress report has shown that based on the ratio of drag to inertial forces two parameters are found to be useful in relating particles in hot gas and cold gas flow fields. These parameters are shown to be valid similarity parameters, within restrictions based on the average Reynolds number of the particle along its trajectory. For Reynolds number above 500, the similarity parameter is the characteristic length, as given in Equation (13). For particles that have Reynolds number generally below one, the similarity parameter is a time constant, as given by Equation (16).

In addition, the characteristic length can be used to study trends in the erosive particle trajectories, even when the Reynolds number is below 500. This is true because even though there is a slight deviation in the similar trajectories, the general pattern of the trajectories does not tend to change significantly when δ^* is the same for two different particles.

These results are applicable to flows in both stationary and rotating reference frames as occur in stator and rotor blades of turbomachinery.

Application to High Speed Photography

One reason for studying the parameters that can be used to determine similar particle trajectories in equivalent hot and cold air turbines is for the purpose of using trajectory data taken with high speed photography. Generally, better photographic data can be obtained with the use of slower gas velocities, larger particle diameters, and higher speed motion picture or flash tube systems. The cold air equivalent turbine provides the slower gas velocities, and the high speed motion picture and flat tube systems are capable of yielding data of sufficient quality to describe the trajectories, if the particle can be distinguished after the film is developed.

Practical experience has indicated that white particles against a black background can be seen with moderately high speed cameras, in the 40,000 picture per second range, if the particles have diameters greater than about 100 microns. Higher speed motion picture systems would require correspondingly larger diameter particles. No data is presently available on the particle size versus repeated flash speed of zenon tube systems, but such systems can be expected to allow the trajectories of small diameter particles to be traced.

As an example of the types of particles that would be required, Table 5 gives the sizes of particles that would be required to simulate SAE Standard Coarse Dust in a cold gas equivalent turbine. The hot gas turbine was assumed to have a stagnation inlet density of

twice the standard sea level density. This would correspond to a stagnation inlet pressure of about 8 atmospheres with an inlet stagnation temperature of about 1155.5°K. The characteristic length, δ^*, indicated for the hot gas case is based on the critical gas density, because this density is the most typical of high speed turbine flows. The table shows that in order to realistically study the particle trajectories in the cold air equivalent case, the particles used would have to have specific gravities less than about 1.0, if they are to be sufficiently large for photographic observation.

It can be noted here that turbines with smaller pressure ratios will have correspondingly larger particle characteristic lengths, δ^*, with correspondingly larger diameter "similar particles" in the equivalent cold air turbine. These diameters and densities are not unrealistic, and with proper selection of similar particles, the complete spectrum of dust can be obtained.

CONCLUSIONS

Similarity parameters have been obtained which allow the determination of erosive particle trajectories for hot air radial inflow turbines from data obtained from cold air turbine tests.

Based on the ratio of drag to inertial forces two parameters are found to be useful in relating particles in hot gas and cold gas flow fields. These parameters are shown to be valid similarity parameters, within restrictions based on the average Reynolds number of the particle along its trajectory. In addition, one of the similarity parameters, a characteristic length, can be used to study trends in the erosive particle trajectories, even when the Reynolds number is generally below 500. This is true because even though there is a slight deviation in the similar trajectories, the general pattern of the trajectories does not tend to change significantly when the characteristic length is held constant.

These results are applicable to flows in both stationary and rotating reference frames as occur in stator and rotor blades of turbomachinery.

In addition, an example of typical particle sizes that can be used to simulate the trajectories of similar particles in an equivalent cold air turbine is presented.

REFERENCES

1. W. Tabakoff and M.F. Hussein, "The Comparison Between Theoretical and Experimental Pressure Distribution on a Blade in Cascade Nozzle for a Particulate Gas Flow." AIAA Paper No. 71-82, Jan. 1971.
2. W. Tabakoff and M.F. Hussein, "Trajectories of Particles Suspended in Fluid Flow Through Cascades," Journal of Aircraft, Vol. 8, No. 1, Jan. 1971.
3. W. Tabakoff and M.F. Hussein, "Properties and Particle Trajectories of a Gas Particle Flow in Cascades," AIAA Paper No. 70-712, June 1970.
4. M.F. Hussein, The Dynamic Characteristics of Solid Particles in Particulate Flow in Rotating Turbomachinery, Ph.D., Thesis University of Cincinnati, 1972.
5. M.F. Hussein and W. Tabakoff, "Gas-Particle Suspension
6. Properties on a Blade-to-Blade Stream Surface of a Cascade Nozzle," Project Themis Report No. 70-17, University of Cincinnati, Dec. 1970. AD-715971.
6. G. Grant and W. Tabakoff, "An Experimental Study of Certain Aerodynamic Effects on Erosion," Project Themis Report No. 72-28, University of Cincinnati, July 1972. AD-749286.
7. G. Grant and W. Tabakoff, "A Quasi-Analytical Method for the Calculation of Particle Trajectories," University of Cincinnati Report No. 73-35, Feb. 1973. AD-757724.
8. G. Grant, R. Ball, and W. Tabakoff, "An Experimental Study of the Erosion Rebound Characteristics of High Speed Particles Impacting a Stationary Specimen," Report No. 73-36, Department of Aerospace Engineering, University of Cincinnati, May 1973. AD-760578.
9. G. Grant, A Model to Predict Erosion in Turbomachinery Due to Solid Particles in Particulate Flow, Ph.D. Thesis, University of Cincinnati, June 1973.
10. H.E. Shoemaker and C.P. Shumate, "Techniques for Reducing Sand and Dust Erosion in Small Gas Turbine Engines," SAE Paper No. 700706, Sept. 1970.

11. A.I. Loshkarev, "Erosion Abrasion Theory of the Blade Apparatus of Centripetal Turbines," Translation of an article published in IZVESTIA AKADEMII NAUK SSSR, No. 2, 134-146, Moscow, 1965.
12. M.D. High, E.J. Felderman, and H.F. Lewis, "Acceleration of a Spherical Particle in a Uniform Gas Flow," J. Spacecraft, 1972.
13. Arthur J. Glassman, Ed., Turbine Design and Application, Vol. 1, NASA Sp-290, Lewis Research Center, 1972.

LIST OF SYMBOLS

A	Area - meters^2
$a, \bar{a}$	Acceleration - meters/second^2
C_D	Drag Coefficient
D	Diameter - meters
$\bar{D}$	Drag Force Vector - newtons
$\bar{e}_e, \bar{e}_\theta, \bar{e}_z$	Unit vectors parallel to the coordinate directions in the cylindrical coordinate system
$\bar{F}$	Force Vector - newtons
Δh	Enthalpy drop across the turbine - joule/kilogram
m	Mass - kilogram
N	Rotating Speed - RPM
Re	Reynolds number - $Re = \rho_g D_p V/\mu_g$
r	Radial component of the position vector in the cylindrical coordinate system - meters
$\bar{r}$	Position Vector - meters
T	Temperature - °K
t	Time - seconds
$\bar{V}$	Velocity vector of the gas flow with respect to the particle motion - meters/second
V_r, V_θ, V_z	Scalar components of the velocity vector, $\bar{V}$ - meters/second
v_r, v_θ, v_z	Scalar components of the gas flow with respect to the rotating reference frame - meters/second
$\dot{w}$	Mass Flowrate - kilograms/second

Greek Symbols

δ	Ratio of inlet total pressure to U.S. standard sea level pressure. Also, the characteristic length, given by Equation (13) - meters
$\delta/\delta t$	The time rate of change of a quantity with respect to rotating reference frame - seconds

ε	Function of the ratio of specific heats for a gas that is used in r ating parameters to that using air inlet conditions at U.S. standard sea level conditions.
δ_{cr}	Squared ratio of critical velocity at turbine inlet to critical velocity at U.S. standard sea level temperature.
θ	Angular component of the position vecotr in the cylindrical coordinate system - radians
ρ	Density - kilograms/meter^3
ω	Rotating Velocity - radians/second
τ	Time Constant given in Equation (1) - seconds
μ	Kinematic Viscosity - newtons-second/meter^2

Subscripts

p	Represents particle property
g	Represents gas property
cr	Represents property evaluated at critical condition
r	Component in the radial direction
θ	Component in the tangential direction
z	Component in the axial direction

Superscripts & Other Symbols

*	Represents properties evaluated at critical conditions
-	Bar - Indicates vector quantity

TABLE 1. PARAMETER VARIATION USED IN TRAJECTORY STUDY FOR FIGURE 4.

Trial No.	Gas Total Temp ^{o}K	Gas Total Density kg/m^3	Particle Specific Gravity	Particle Diameter Microns	Characteristic Length δ^* - cm
1	288.3	1.224	10.00	10	42.7
2	288.3	1.224	2.00	50	42.7
3 Ref.	288.3	1.224	1.00	100	42.7
4	288.3	1.224	0.20	500	42.7
5	288.3	1.224	0.10	1000	42.7
6	288.3	0.801	1.00	65	42.7
7	288.3	1.602	1.00	131	42.7
8	288.3	2.403	1.00	196	42.7
9	288.3	3.204	1.00	262	42.7
10	288.3	4.005	1.00	327	42.7
11	288.3	0.801	0.65	100	42.7
12	288.3	1.602	1.31	100	42.7
13	288.3	2.403	1.96	100	42.7
14	288.3	3.204	2.62	100	42.7
15	288.3	4.005	3.27	100	42.7
16	1111.1	3.186	0.25	1000	42.7
17	1111.1	3.186	0.50	500	42.7
18	1111.1	3.186	5.00	50	42.7
19	1111.1	0.801	1.00	65	42.7
20	1111.1	1.602	1.00	131	42.7
21	1111.1	2.403	1.00	196	42.7
22	1111.1	3.204	1.00	262	42.7
23	1111.1	4.005	1.00	327	42.7
24	1111.1	0.801	0.65	100	42.7
25	1111.1	1.602	1.31	100	42.7
26	1111.1	2.403	1.96	100	42.7
27	1111.1	3.204	2.62	100	42.7
28	1111.1	4.005	3.27	100	42.7

TABLE 2. PARAMETER VARIATION USED IN TRAJECTORY STUDY FOR FIGURE 6.

Trial No.	Gas Total Temp ^{o}K	Gas Total Density kg/m^3	Particle Specific Gravity	Particle Diameter Microns	Characteristic Length δ^* - cm
1	1111.1	3.186	10.00	10	16.5
2	1111.1	3.186	2.00	50	16.5
3 Ref.	1111.1	3.186	1.00	100	16.5
4	1111.1	3.186	0.20	500	16.5
5	1111.1	3.186	0.10	1000	16.5
6	1111.1	0.801	1.00	25	16.5
7	1111.1	1.602	1.00	50	16.5
8	1111.1	2.403	1.00	75	16.5
9	1111.1	3.204	1.00	100	16.5
10	1111.1	4.005	1.00	126	16.5
11	1111.1	0.801	0.25	100	16.5
12	1111.1	1.602	0.50	100	16.5
13	1111.1	2.403	0.75	100	16.5
14	1111.1	3.204	1.00	100	16.5
15	1111.1	4.005	1.26	100	16.5
16	288.3	1.224	0.04	1000	16.5
17	288.3	1.224	0.08	500	16.5
18	288.3	1.224	0.77	50	16.5
19	288.3	1.224	3.81	10	16.5
20	288.3	0.801	1.00	25	16.5
21	288.3	1.602	1.00	50	16.5
22	288.3	2.403	1.00	75	16.5
23	288.3	3.204	1.00	100	16.5
24	288.3	4.005	1.00	126	16.5
25	288.3	0.801	0.25	100	16.5
26	288.3	1.602	0.50	100	16.5
27	288.3	2.403	0.75	100	16.5
28	288.3	3.204	1.00	100	16.5
29	288.3	4.005	1.26	100	16.5

TABLE 3. PARAMETER VARIATION USED IN TRAJECTORY STUDY FOR FIGURE 8.

Trial No.	Gas Total Temperature ^{o}K	Gas Total Density kg/m^3	Gas Critical Viscosity n sec/m^2	Particle Specific Gravity	Particle Diameter Microns	Time Constant τ^* sec
1	1111.1	3.186	3.72×10^{-5}	1.00	1.00	1.47×10^{-7}
2	288.3	1.224	1.42×10^{-5}	0.38	1.00	1.47×10^{-7}
3	288.3	1.224	1.42×10^{-5}	1.00	0.61	1.47×10^{-7}
4	288.3	0.801	1.42×10^{-5}	0.38	1.00	1.47×10^{-7}
5	288.3	1.602	1.42×10^{-5}	0.38	1.00	1.47×10^{-7}
6	288.3	2.403	1.42×10^{-5}	0.38	1.00	1.47×10^{-7}
7	288.3	3.204	1.42×10^{-5}	0.38	1.00	1.47×10^{-7}
8	288.3	4.005	1.42×10^{-5}	0.38	1.00	1.47×10^{-7}
9	288.3	0.801	1.42×10^{-5}	1.00	0.61	1.47×10^{-7}
10	288.3	1.602	1.42×10^{-5}	1.00	0.61	1.47×10^{-7}
11	288.3	2.403	1.42×10^{-5}	1.00	0.61	1.47×10^{-7}
12	288.3	3.204	1.42×10^{-5}	1.00	0.61	1.47×10^{-7}
13	288.3	4.005	1.42×10^{-5}	1.00	0.61	1.47×10^{-7}

TABLE 4. PARAMETER VARIATION USED IN TRAJECTORY STUDY FOR FIGURE 9.

Trial No.	Gas Total Temperature ^{o}K	Gas Total Density kg/m^3	Gas Critical Viscosity n sec/m^2	Particle Specific Gravity	Particle Diameter Microns	Time Constant τ^* - sec
1	1111.1	3.186	3.72×10^{-5}	1.05	10.0	1.57×10^{-4}
2	288.3	1.224	1.42×10^{-5}	0.40	10.0	1.57×10^{-4}
3	288.3	1.224	1.42×10^{-5}	1.00	6.3	1.57×10^{-4}
4	288.3	0.801	1.42×10^{-5}	0.40	10.0	1.57×10^{-4}
5	288.3	1.602	1.42×10^{-5}	0.40	10.0	1.57×10^{-4}
6	288.3	2.403	1.42×10^{-5}	0.40	10.0	1.57×10^{-4}
7	288.3	3.204	1.42×10^{-5}	0.40	10.0	1.57×10^{-4}
8	288.3	4.005	1.42×10^{-5}	0.40	10.0	1.57×10^{-4}
9	288.3	0.801	1.42×10^{-5}	1.00	6.3	1.57×10^{-4}
10	288.3	1.602	1.42×10^{-5}	1.00	6.3	1.57×10^{-4}
11	288.3	2.403	1.42×10^{-5}	1.00	6.3	1.57×10^{-4}
12	288.3	3.204	1.42×10^{-5}	1.00	6.3	1.57×10^{-4}
13	288.3	4.005	1.42×10^{-5}	1.00	6.3	1.57×10^{-4}

TABLE 5. SIMILAR PARTICLES FOR VISUAL STUDIES OF EROSIVE PARTICLE TRAJECTORIES

SAE St'd Course Grade Dust				Characteristic Length, δ^*, For Hot Gas $\rho/\rho_{St'd} = 2.0$	Corresponding Particle Size in Cold Air Equivalent Flow For Various Densities			
	% by wt				DIAMETERS IN MICRONS			
					PARTICLE SPECIFIC GRAVITIES			
Particle Type	Mixture	Size	Diameter Microns	cm	1.2	1.0	0.8	0.6
SiO_2	70%	10%	80-	13.7	88-	106-	132-	177-
		30%	40-80	6.83-13.7	44-88	53-106	66-132	88-177
		20%	20-40	3.41- 6.83	22-44	26-53	33-66	44-88
		40%	0-20	0 - 3.41	0-22	0-26	0-33	0-44
Al_2O_3	20%	10%	80-	13.7	132-	159-	199-	265-
		30%	40-80	6.83-13.7	66-132	79-159	99-199	133-265
		20%	20-40	3.41- 6.83	33-66	40-79	50-99	66-133
		40%	0-20	0 - 3.41	0-33	0-40	0-50	0-66
Fe_2O_3	5%	10%	80-	13.7	173-	209-	262-	348-
		30%	40-80	6.83-13.7	87-173	104-209	130-262	173-348
		20%	20-40	3.41- 6.83	39-87	52-104	65-130	87-173
		40%	0-20	0 - 3.41	0-39	0-52	0-63	0-87

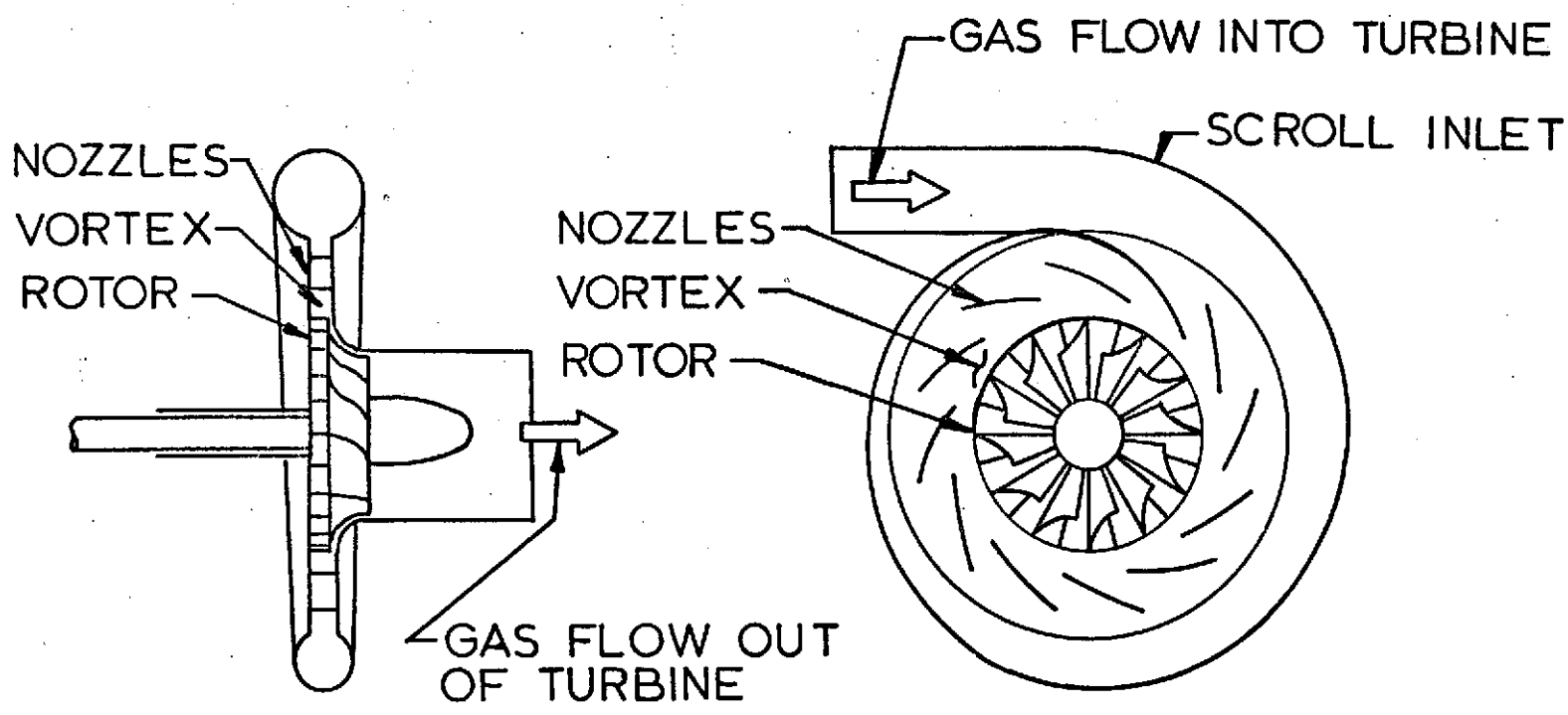

FIGURE 1. SCHEMATIC OF TYPICAL RADIAL INFLOW TURBINE.

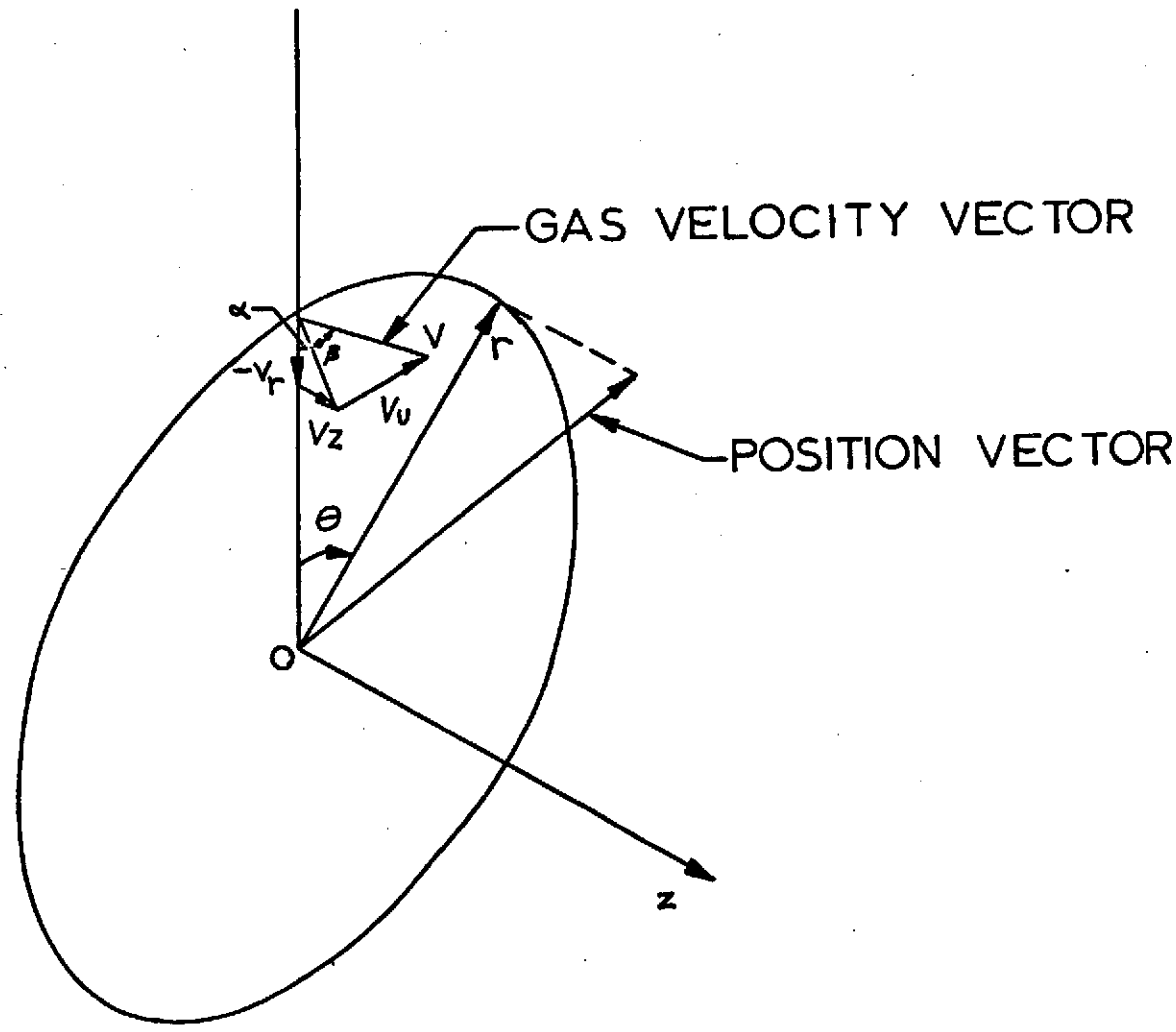

FIGURE 2. COORDINATE SYSTEM AND TYPICAL GAS VELOCITY COMPONENTS.

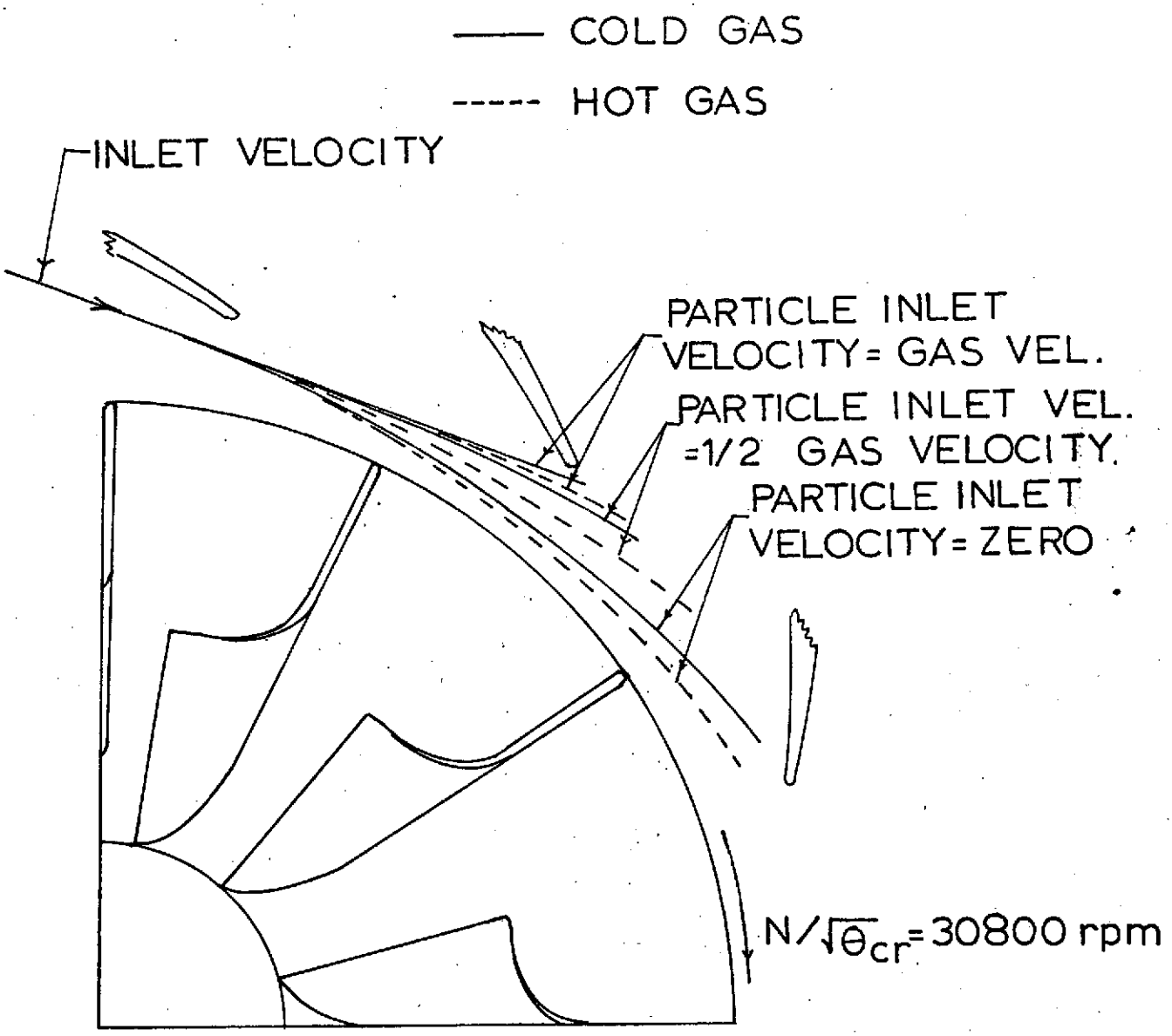

FIGURE 3 VARIATION OF TRAJECTORIES WITH PARTICLE INLET VELOCITIES FOR 100 MICRON PARTICLES.

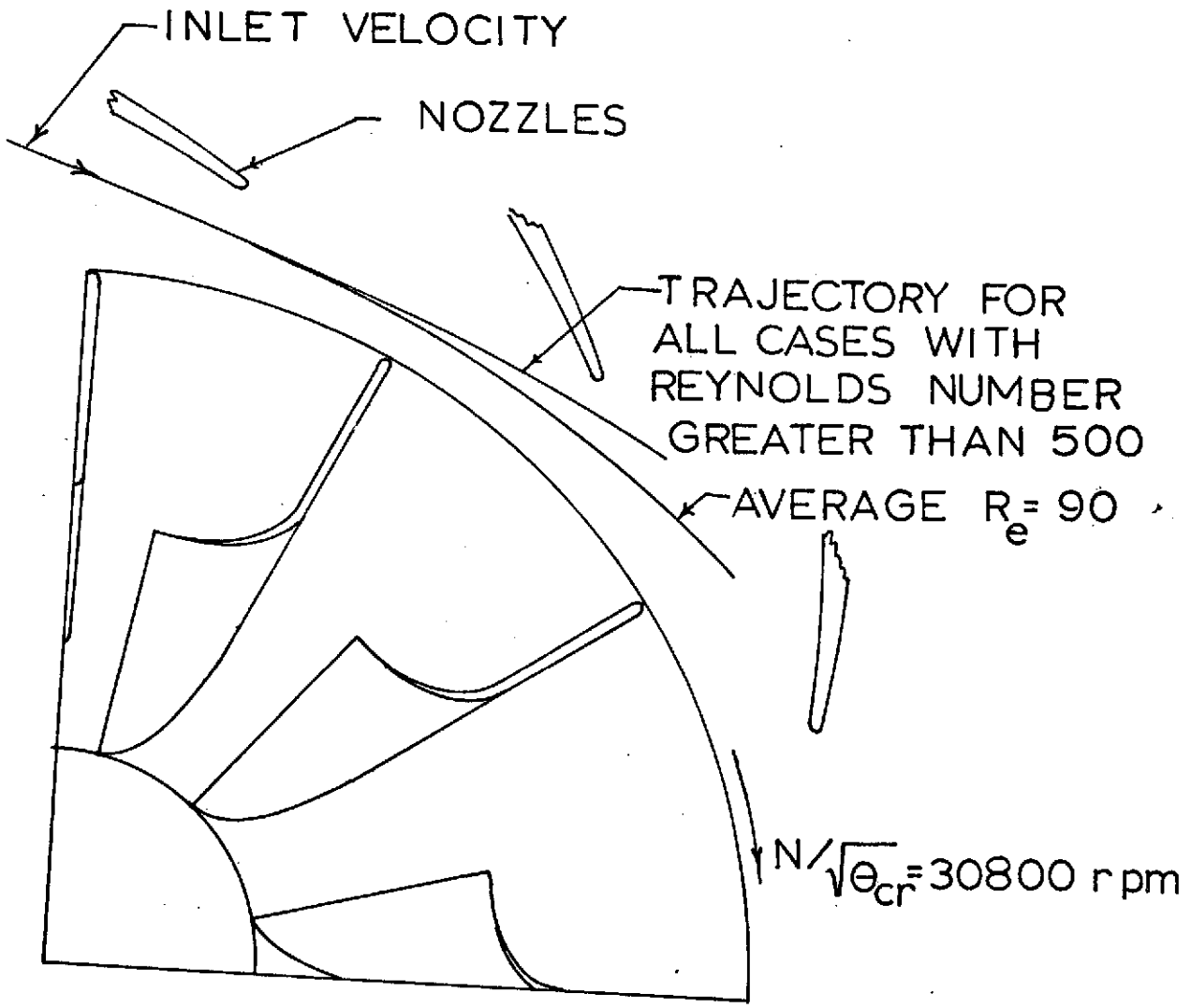

FIGURE 4 TRAJECTORIES OF PARTICLES WITH CHARACTERISTIC LENGTH EQUAL TO 42.6 cm

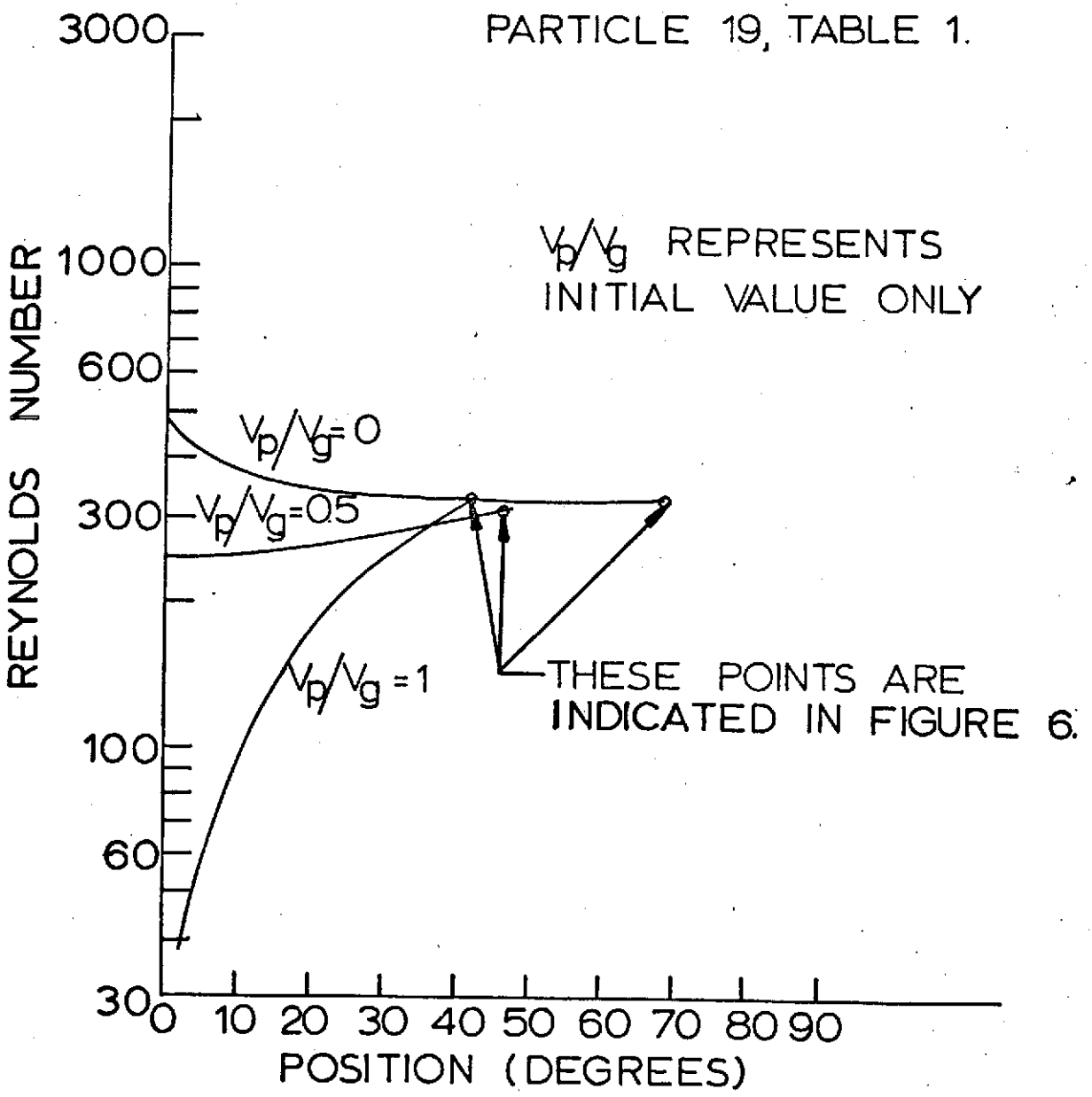

FIGURE 5. REYNOLDS NUMBER VARIATION ALONG PARTICLE TRAJECTORY IN VORTEX.

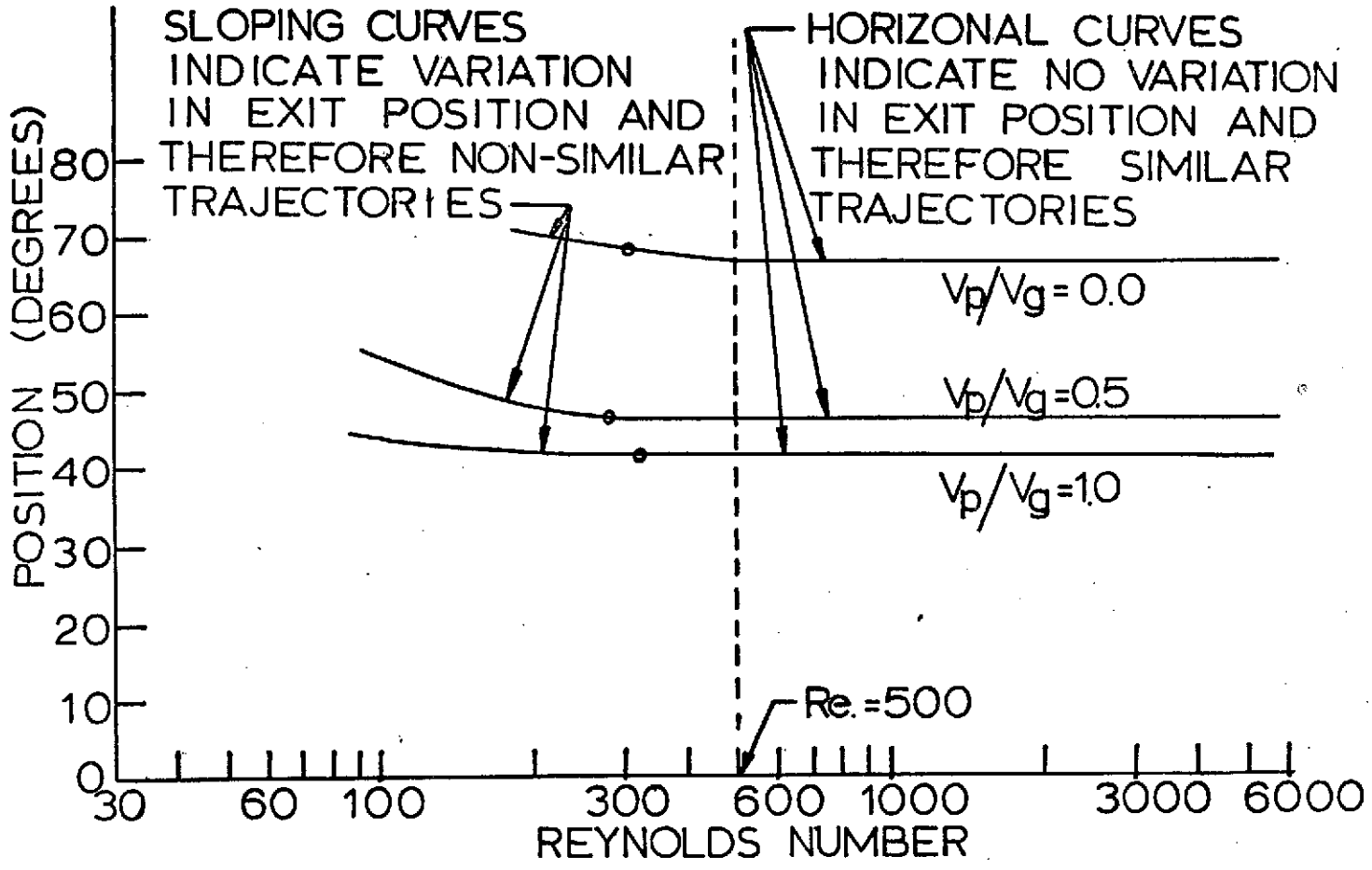

FIGURE 6. EXIT POSITION VARIATION WITH REYNOLDS NUMBER

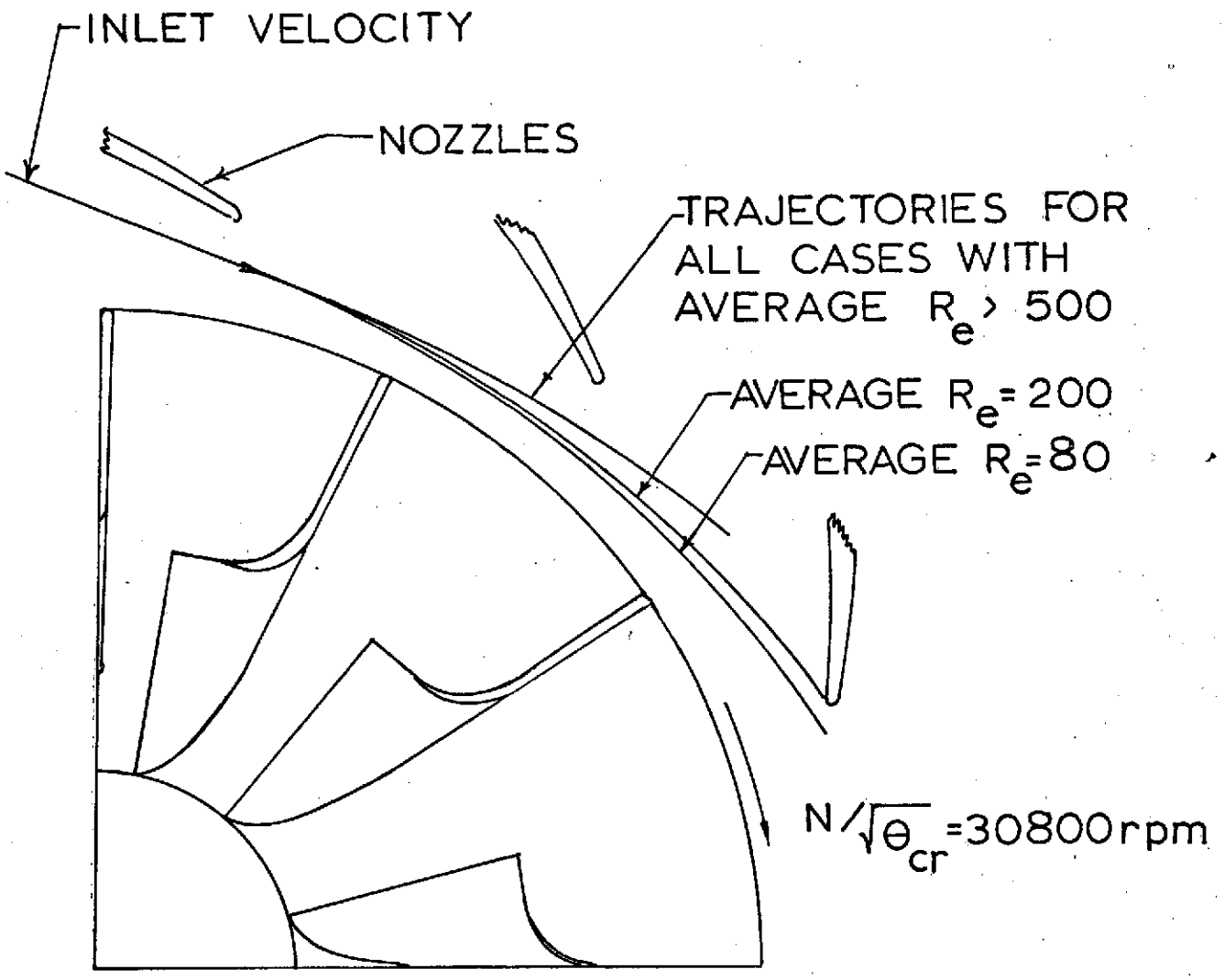

FIGURE 7 TRAJECTORIES OF PARTICLES WITH CHARACTERISTIC LENGTH EQUAL TO 16.5 cm.

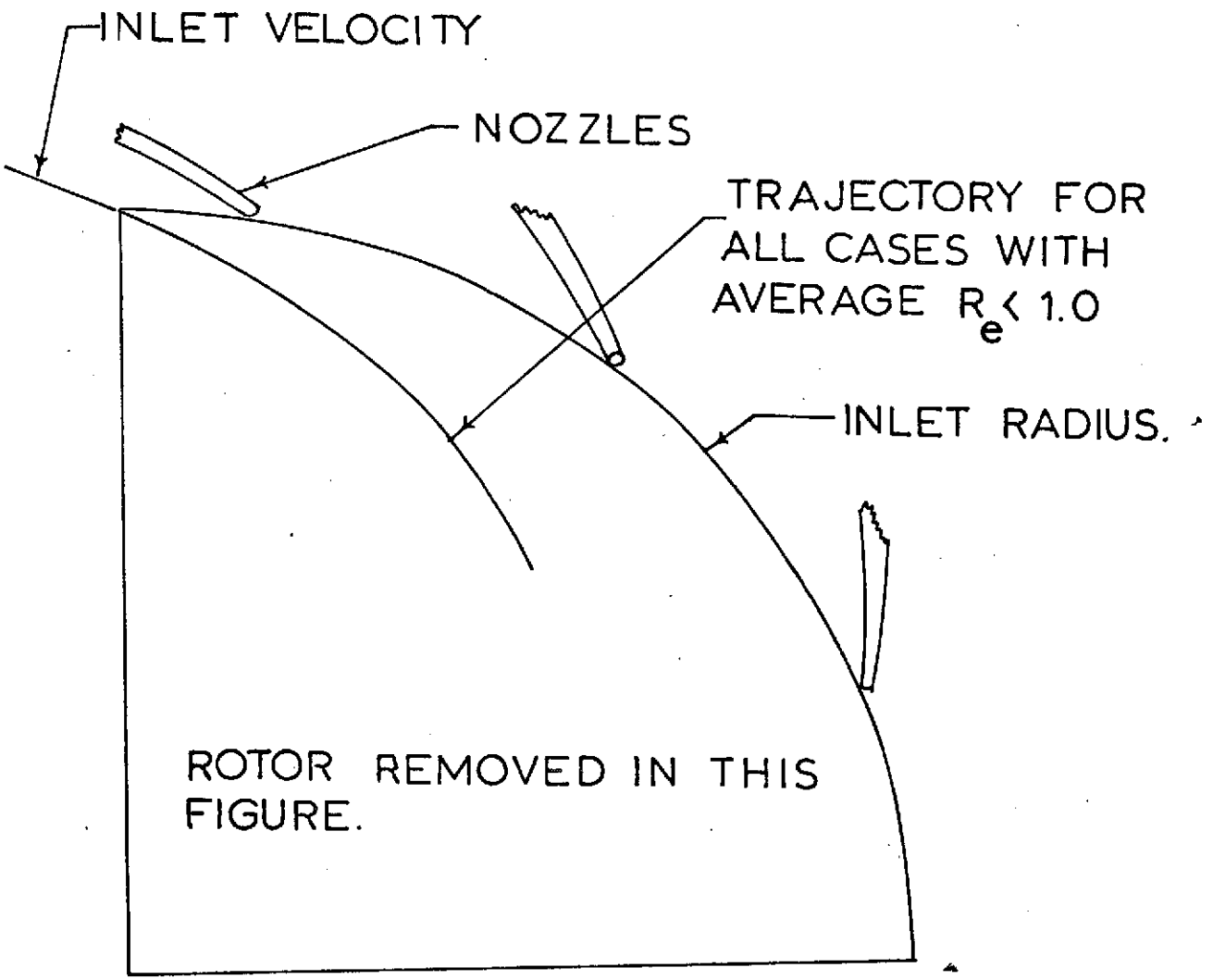

FIGURE 8 TRAJECTORIES OF PARTICLES WITH TIME CONSTANT $= 1.47 \times 10^{-7}$ sec.

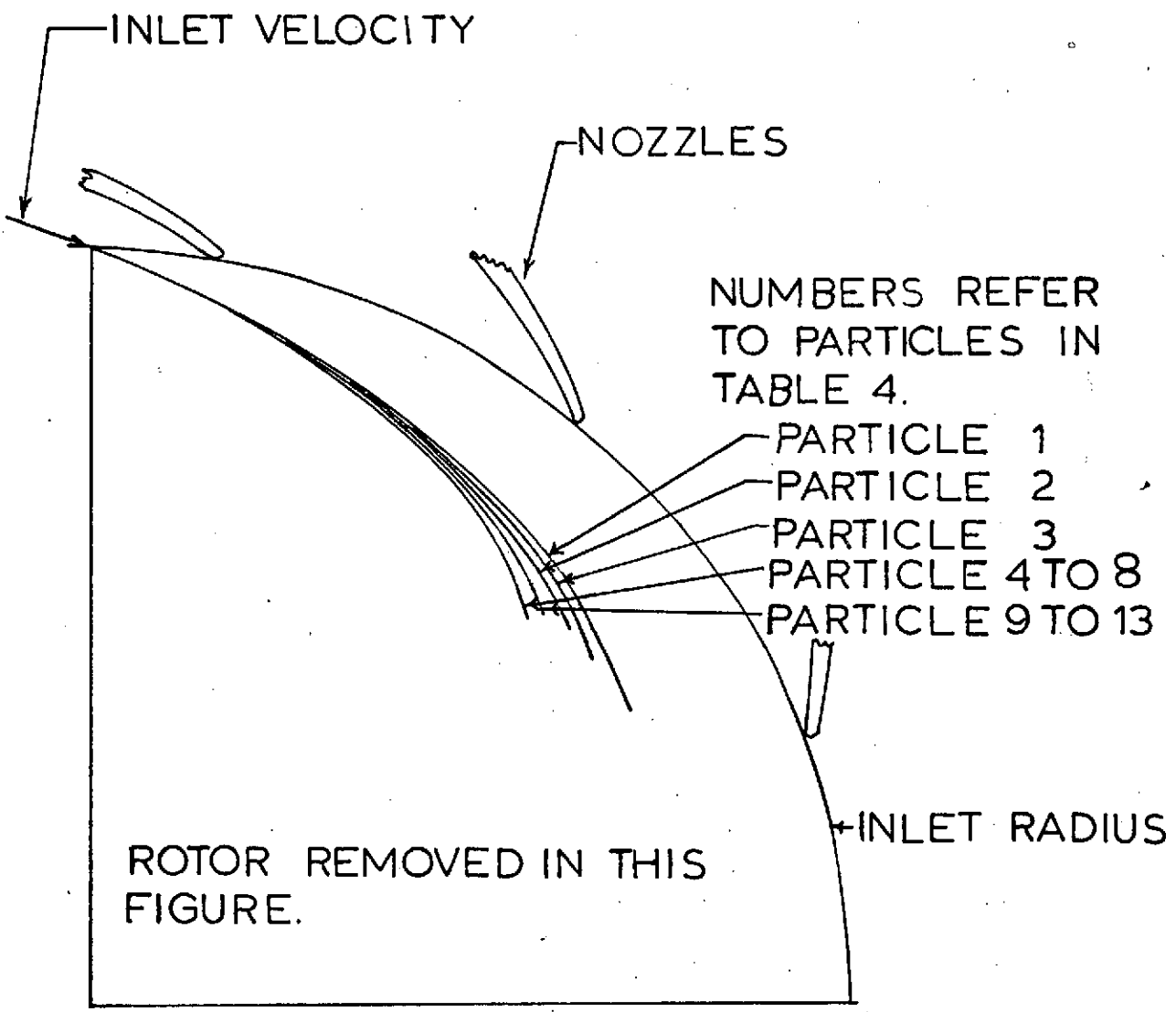

FIGURE 9 TRAJECTORIES OF PARTICLES WITH TIME CONSTANT = 1.57×10^{-4} sec.

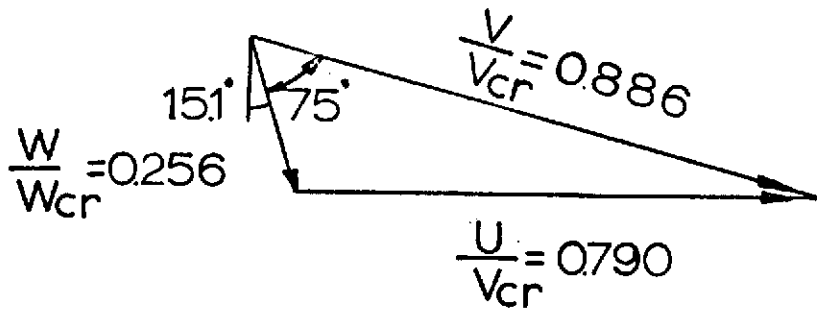

TIP

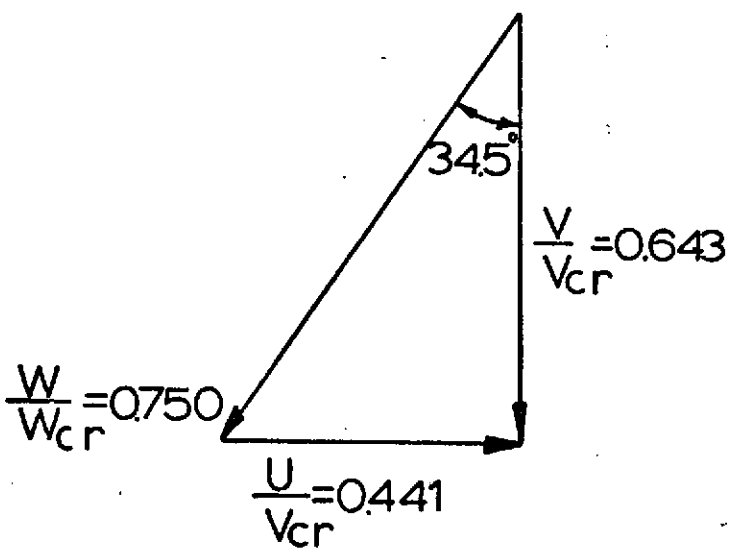

EXIT MEAN

FIGURE 10 VELOCITY DIAGRAMS FOR ROTOR

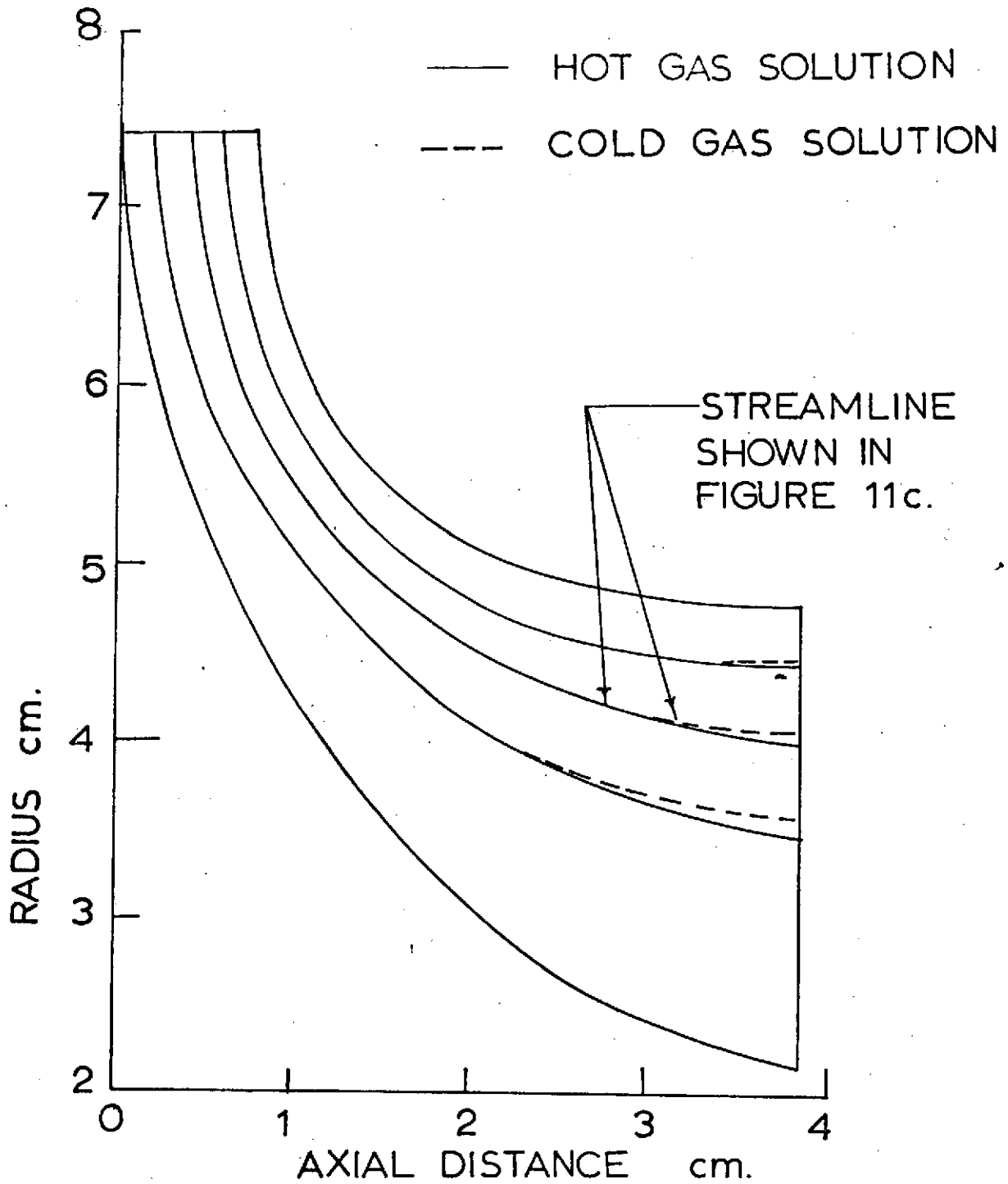

FIGURE 11a MERIDIONAL VIEW OF ROTOR

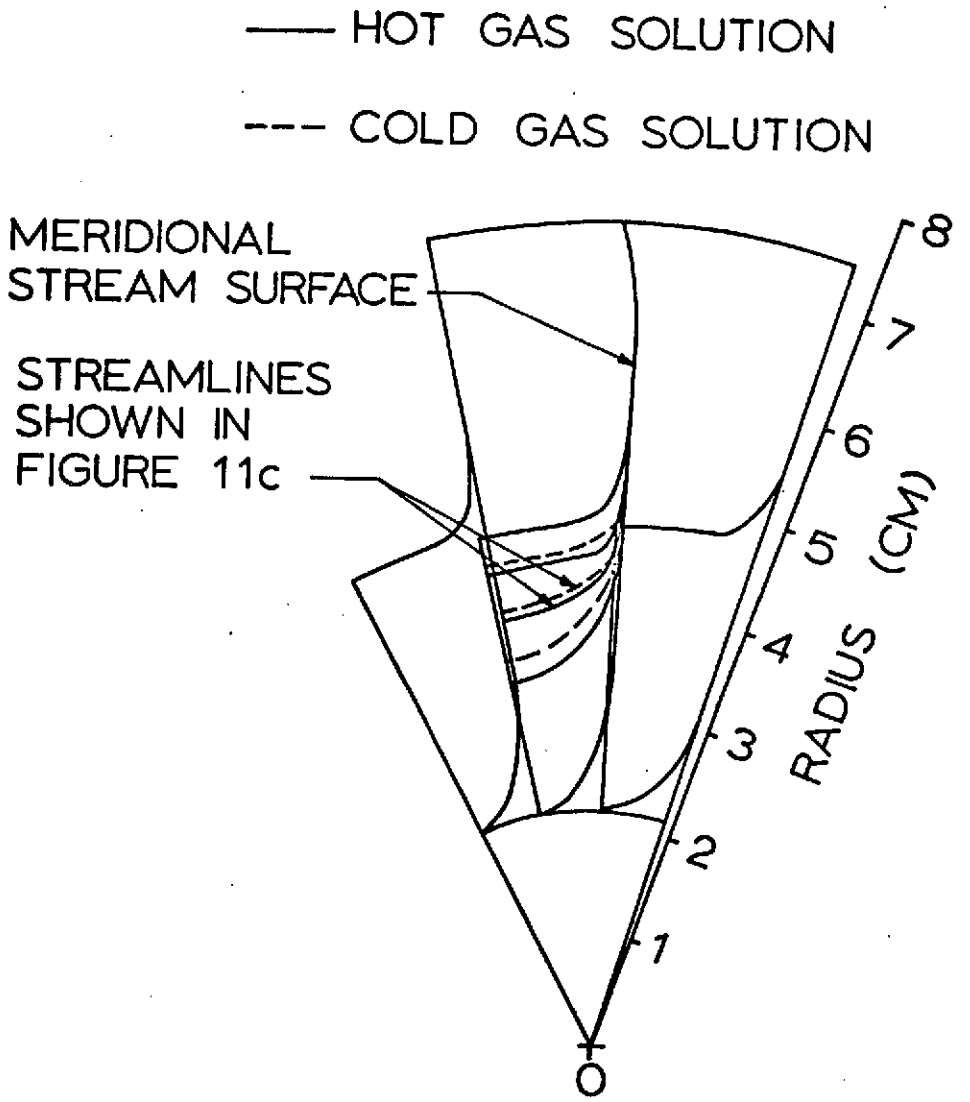

FIGURE 11b. AXIAL VIEW OF ROTOR WITH RESPECT TO ROTATING REFERENCE FRAME.

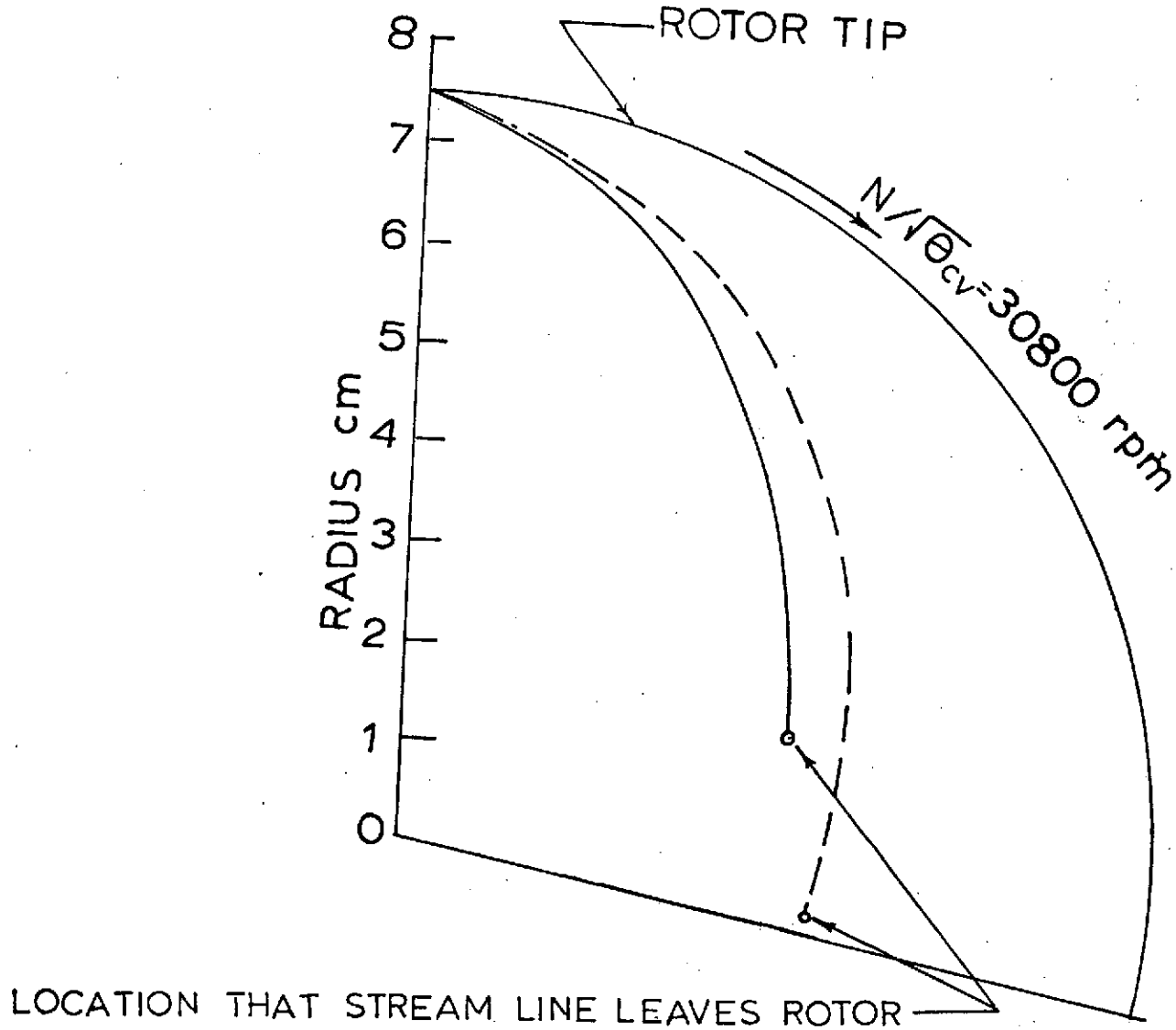

FIGURE 11c AXIAL VIEW OF ROTOR WITH RESPECT TO NON-ROTATING REFERENCE FRAME.

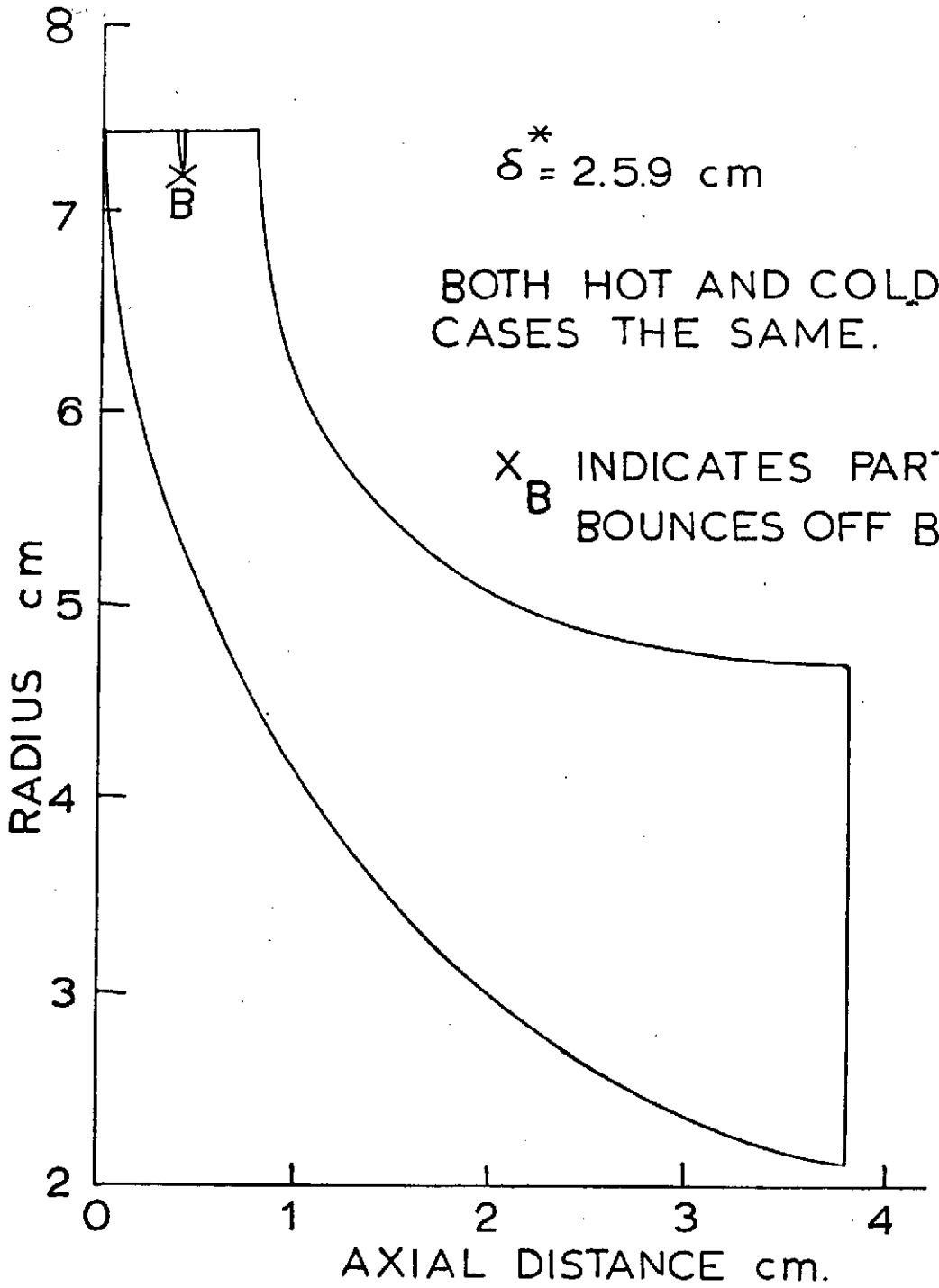

FIGURE 12a MERIDIONAL VIEW OF PARTICLE TRAJECTORIES IN ROTOR.

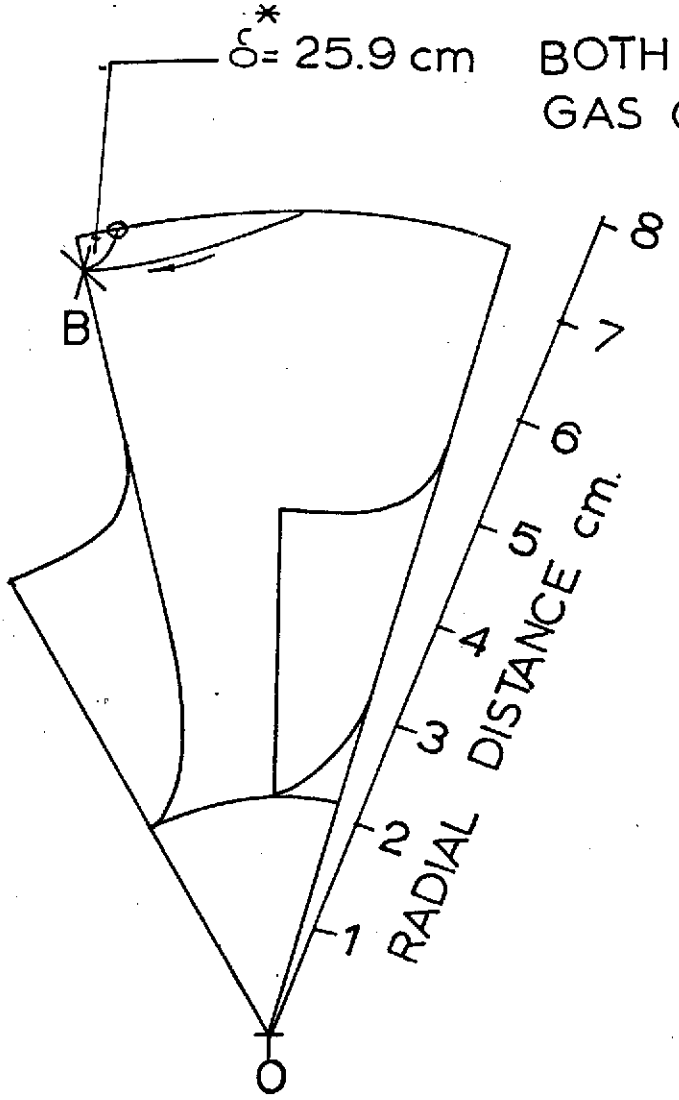

BOTH HOT GAS AND COLD GAS CASES.

X_B INDICATES BOUNCE OFF BLADE.

∘ INDICATES LOCATION THAT PARTICLE LEAVES ROTOR.

FIGURE 12 b

AXIAL VIEW OF PARTICLE TRAJECTORIES IN ROTOR, WITH RESPECT TO ROTATING REFERENCE FRAME.

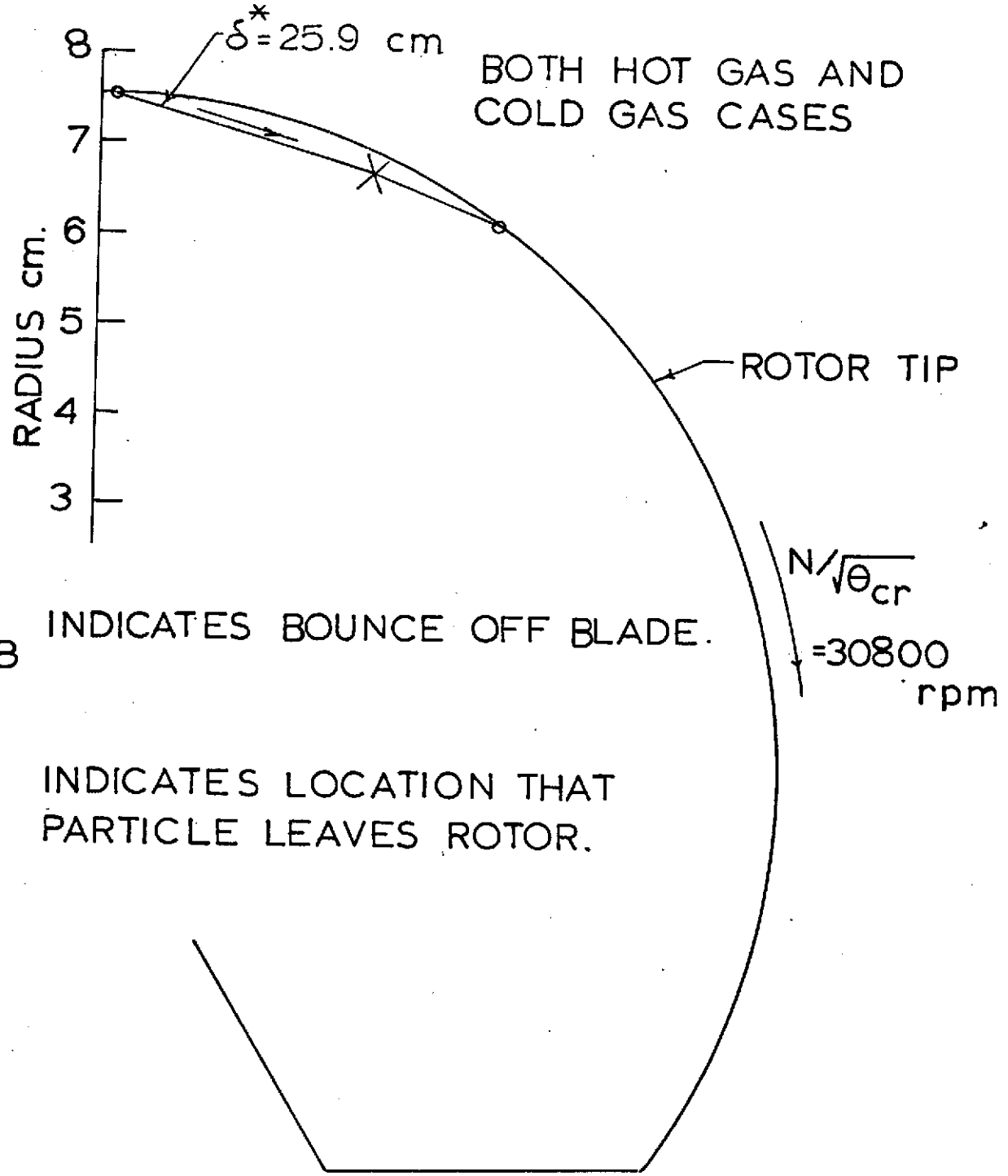

FIGURE 12c AXIAL VIEW OF PARTICLE TRAJECTORIES IN ROTOR WITH RESPECT TO NON-ROTATING REFERENCE FRAME.

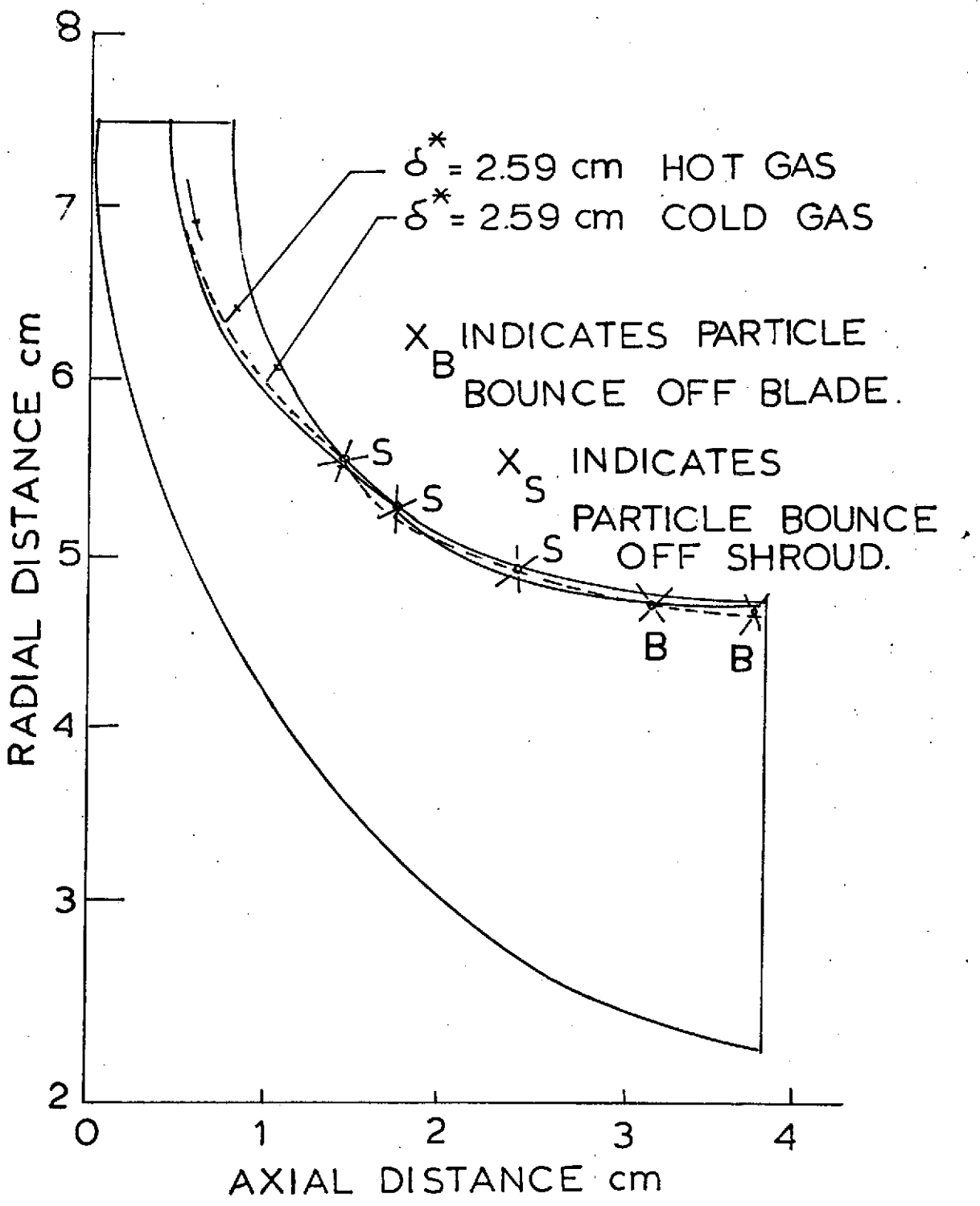

FIGURE 13a MERIDIONAL VIEW OF PARTICLE TRAJECTORIES IN ROTOR.

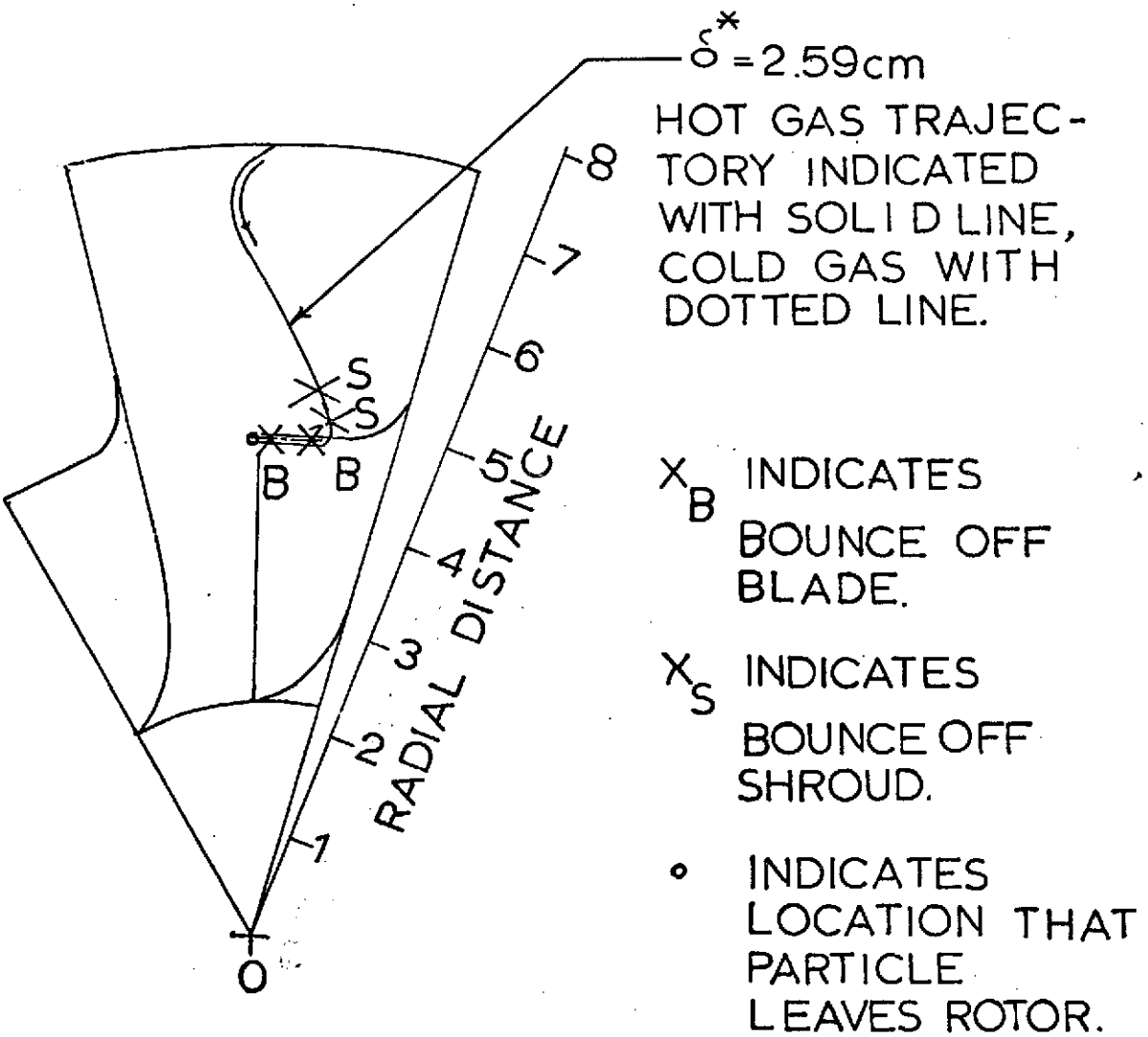

FIGURE 13b AXIAL VIEW OF PARTICLE TRAJECTORIES IN ROTOR, WITH RESPECT TO ROTATING REFERENCE FRAME.

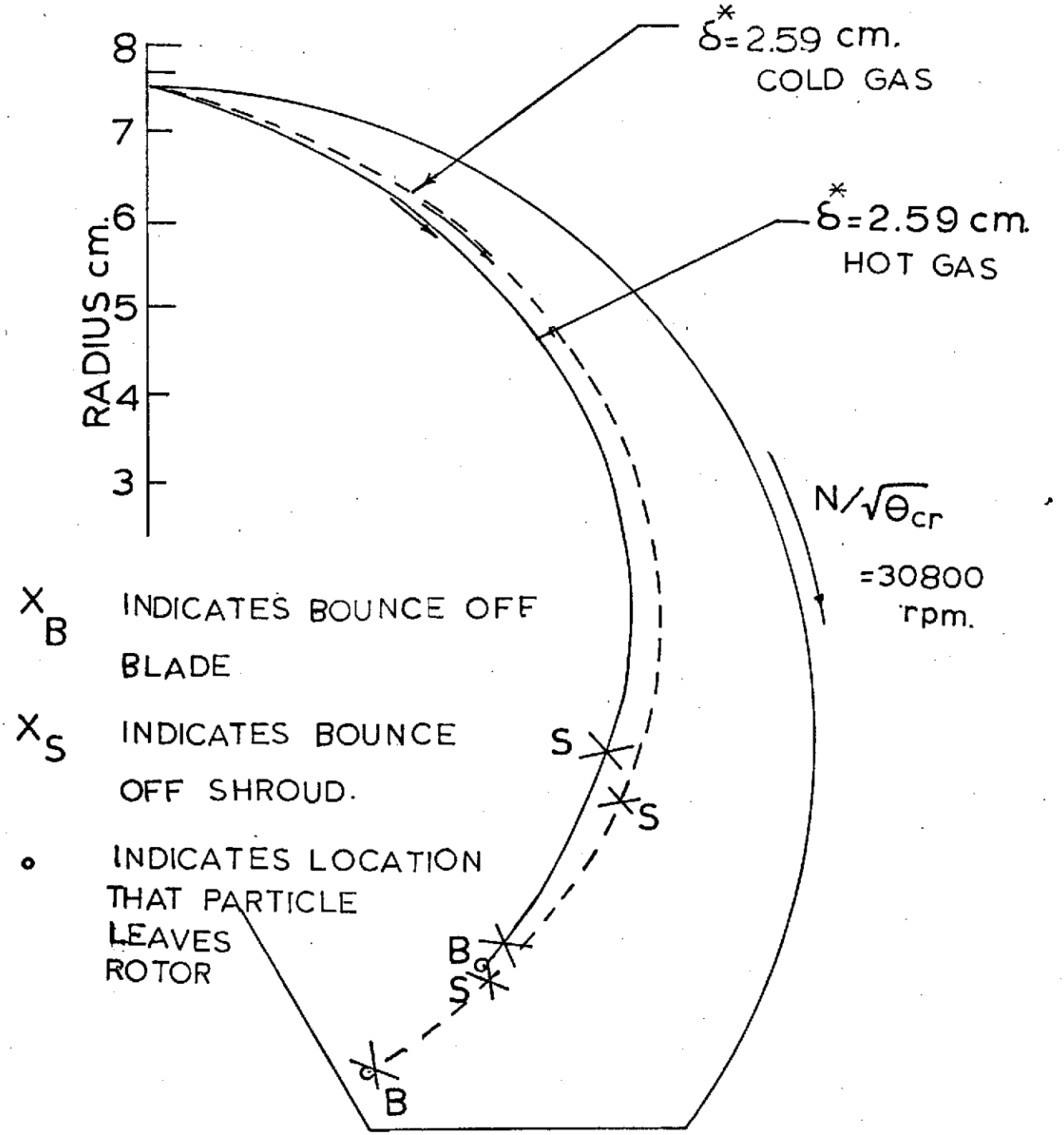

FIGURE 13c AXIAL VIEW OF PARTICLE TRAJECTORIES IN ROTOR, WITH RESPECT TO NON-ROTATING REFERENCE FRAME.

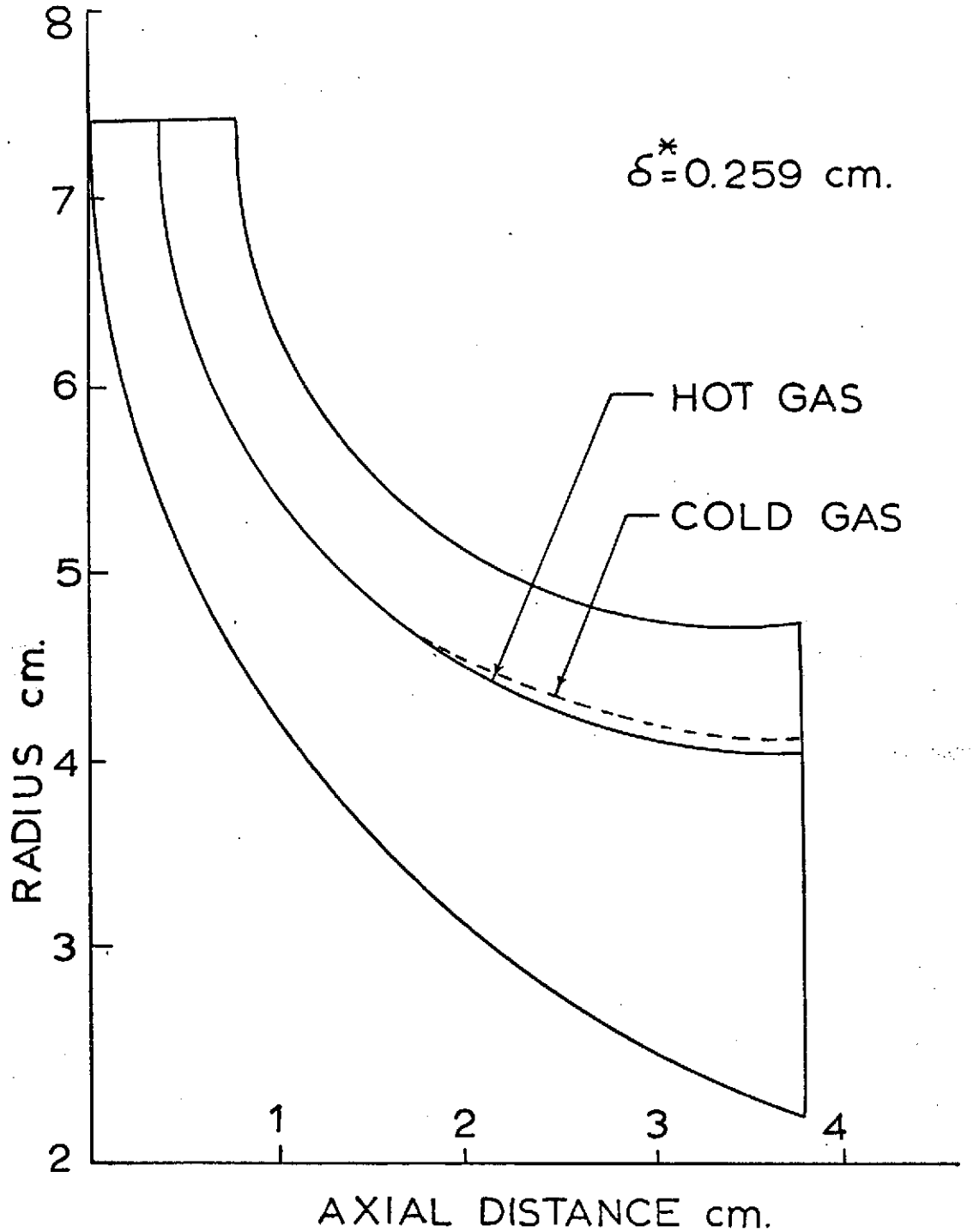

FIGURE 14 a MERIDIONAL VIEW OF TRAJECTORIES OF PARTICLE IN THE ROTOR

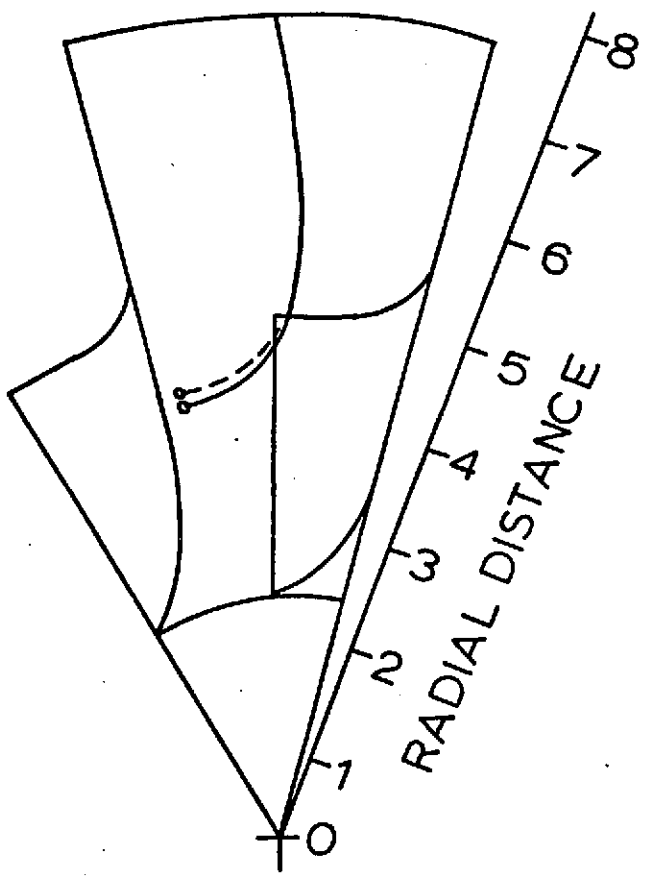

$\delta^* = 0.259$ cm.

HOT GAS TRAJECTORY INDICATED WITH SOLID LINE, COLD GAS WITH DOTTED LINE.

∘ INDICATES LOCATION THAT PARTICLE LEAVES ROTOR

FIGURE 14b. AXIAL TRAJECTORIES OF PARTICLES IN ROTOR, WITH RESPECT TO ROTATING REFERENCE FRAME.

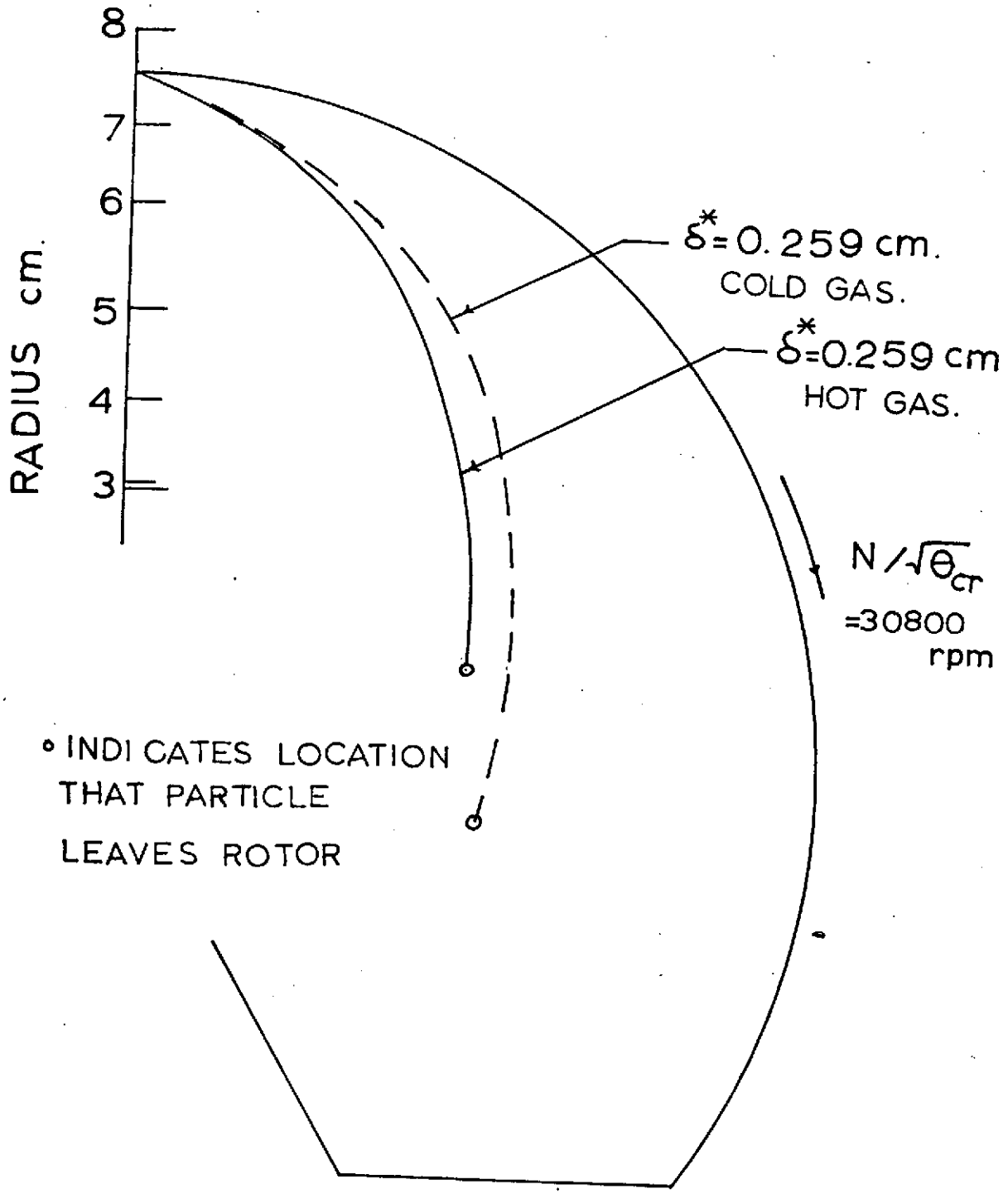

FIGURE 14C

AXIAL VIEW OF PARTICLE TRAJECTORIES IN ROTOR, WITH RESPECT TO NON-ROTATING REFERENCE FRAME.